Reviews in Mineralogy & Geochemistry
Vol. 66, pp. XXX-XXX, 2007

Paleoelevation Reconstruction using Pedogenic Carbonates

Jay Quade
Department of Geosciences
University of Arizona
Tucson, Arizona, 85721, U.S.A.
quadej@email.arizona.edu

Carmala Garzione
Department of Earth and Environmental Sciences
University of Rochester
Rochester, New York, 14627, U.S.A.
garzione@earth.rochester.edu

John Eiler
Division of Geological and Planetary Sciences
California Institute of Technology
Pasadena, California, 91125, U.S.A.
eiler@gps.caltech.edu

ABSTRACT

Paleoelevation reconstruction using stable isotopes, although a relatively new science, is making a significant contribution to our understanding of the recent growth of the world's major orogens. In this review we examine the use of both light stable isotopes of oxygen and the new "clumped-isotope" (Δ_{47}) carbonate thermometer in carbonates from soils. Globally, the oxygen isotopic composition ($\delta^{18}O$) of rainfall decreases on average by about 2.8 ‰/km of elevation gain. This effect of elevation will in turn be archived in the $\delta^{18}O$ value of soil carbonates, and paleoelevation can be reconstructed, provided (1) temperature of formation can be estimated, (2) the effects of evaporation are small, (3) the effects of climate change can be accounted for, and (4) the isotopic composition of the carbonate is not diagenetically altered. We review data from modern soils to evaluate some these issues and find that evaporation commonly elevates $\delta^{18}O$ values of carbonates in deserts, an effect that would lead to underestimates of paleoelevation. Some assessment of paleoaridity, using qualitative indicators or carbon isotopes from soil carbonate, is therefore useful in evaluating the oxygen isotope-based estimates of paleoelevation. Sampling from deep (> 50 cm) in paleosols helps reduce the uncertainties arising from seasonal temperature fluctuations and from evaporation.

The new "clumped-isotope" (Δ_{47}) carbonate thermometer, expressed as Δ_{47}, offers an independent and potentially very powerful approach to paleoelevation reconstruction. In contrast to the use of $\delta^{18}O$ values, nothing need be known about the isotopic composition of water from which carbonate grew in order to estimate of temperature of carbonate formation from Δ_{47} values. Using assumed temperature lapse rates with elevation, paleoelevations can thereby be reconstructed.

Case studies from the Andes and Tibet show how these methods can be used alone or in combination to estimate paleoelevation. In both cases, the potential for diagenetic alteration

1529-6466/07/0066-0003$05.00 DOI: 10.2138/rmg.2007.66.3

of primary carbonate values first has to be assessed. Clear examples of both preservation and alteration of primary isotopic values are available from deposits of varying ages and burial histories. Δ_{47} values constitute a relatively straightforward test, since any temperature in excess of reasonable surface temperatures points to diagenetic alteration. For $\delta^{18}O$ values, preservation of isotopic heterogeneity between different carbonate phases offers a check on diagenesis. Results of these case studies show that one area of south-central Tibet attained elevations comparable to today by the late Oligocene, whereas 2.7 ± 0.4 km of uplift occurred in the Bolivian Altiplano during the late Miocene.

INTRODUCTION

There is considerable debate over the timing and causes of uplift of the earth's great mountain ranges and plateaux, such as Tibet, the Himalaya, and the Andes (Fig. 1). Estimates of paleoelevation change provide key constraints for competing general models that link such large-scale orogenic events with lithospheric-scale geodynamic processes (Currie et al. 2005; Garzione et al. 2006; Rowley and Currie 2006; Kent-Corson et al. 2007). The use of the isotopic composition of carbonates, silicates, and oxides is at the forefront of these paleoelevation reconstructions. In this chapter we review use of one of several geologically abundant secondary carbonates—calcite formed in soils (or "pedogenic carbonate")—in paleoelevation reconstruction.

The H and O isotopic composition of rainfall (expressed as $\delta^{18}O_{mw}$ and δD_{mw} values in per mil, or ‰, relative to SMOW) varies primarily as a function of the degree of rainout (removal of water condensate) from a vapor mass. As rainout proceeds, ^{2}H (D) and ^{18}O are preferentially removed from the vapor mass, decreasing δD and $\delta^{18}O$ values of both the water vapor and rainfall derived from it. As a vapor mass ascends over mountains, adiabatic expansion causes cooling and condensation of water as so-called "orographic precipitation" (e.g., Roe 2005), producing some of the largest isotopic gradients in rainfall observed on Earth. A number of studies document large fractionations in the H and O isotopes in rainfall, snowfall, and associated surface water with increasing elevation (e.g., Ambach et al. 1968; Siegenthaler and Oeschger 1980; Rozanski and Sonntag 1982, Ramesh and Sarin 1995; Garzione et al. 2000a; Gonfiantini et al. 2001; Stern and Blisniuk 2002; Rowley and Garzione 2007; but see Dutton et al. 2005). The $\delta^{18}O$-elevation relationship has been calibrated both empirically (e.g., Garzione et al. 2000a, Poage and Chamberlain 2001) and theoretically using basic thermodynamic principles that govern isotopic fractionation of an ascending vapor mass (Rowley et al. 2001; Rowley and Garzione 2007). Globally, the $\delta^{18}O_{mw}$ value of rainfall on average decreases by 2.8 ‰/km (Poage and Chamberlain 2001), although the scatter around this average is very considerable (Blisniuk and Stern 2005), as we discuss for the cases of Tibet and the Andes in the next section of this review.

Studies using oxygen (and hydrogen) isotopes take advantage of this strong sensitivity of $\delta^{18}O_{mw}$ values to elevation change to reconstruct paleoelevation. Stated simply, the basic approach to paleoelevation reconstruction is this: the oxygen isotope composition of paleocarbonate buried in geologic sections can be used to estimate the oxygen isotope composition of soil water, which in turn is used as an estimate of $\delta^{18}O_{mw}$ values; and it is this estimate of $\delta^{18}O_{mw}$ values that is compared with empirical or theoretical isotopic lapse rates to estimate paleoelevation.

Two key complications in this approach to paleoelevation reconstruction are that carbonates, including pedogenic carbonate which forms in soils, record the oxygen isotopic composition of soil waters (which may differ from meteoric water) *and* of the temperature of carbonate formation, both of which vary with elevation. Early studies used the $\delta^{18}O$ value of pedogenic carbonates (or $\delta^{18}O_{sc}$, expressed in ‰ relative to PDB) to reconstruct elevation by assuming temperatures of formation that allowed calculation of the $\delta^{18}O$ value of soil water

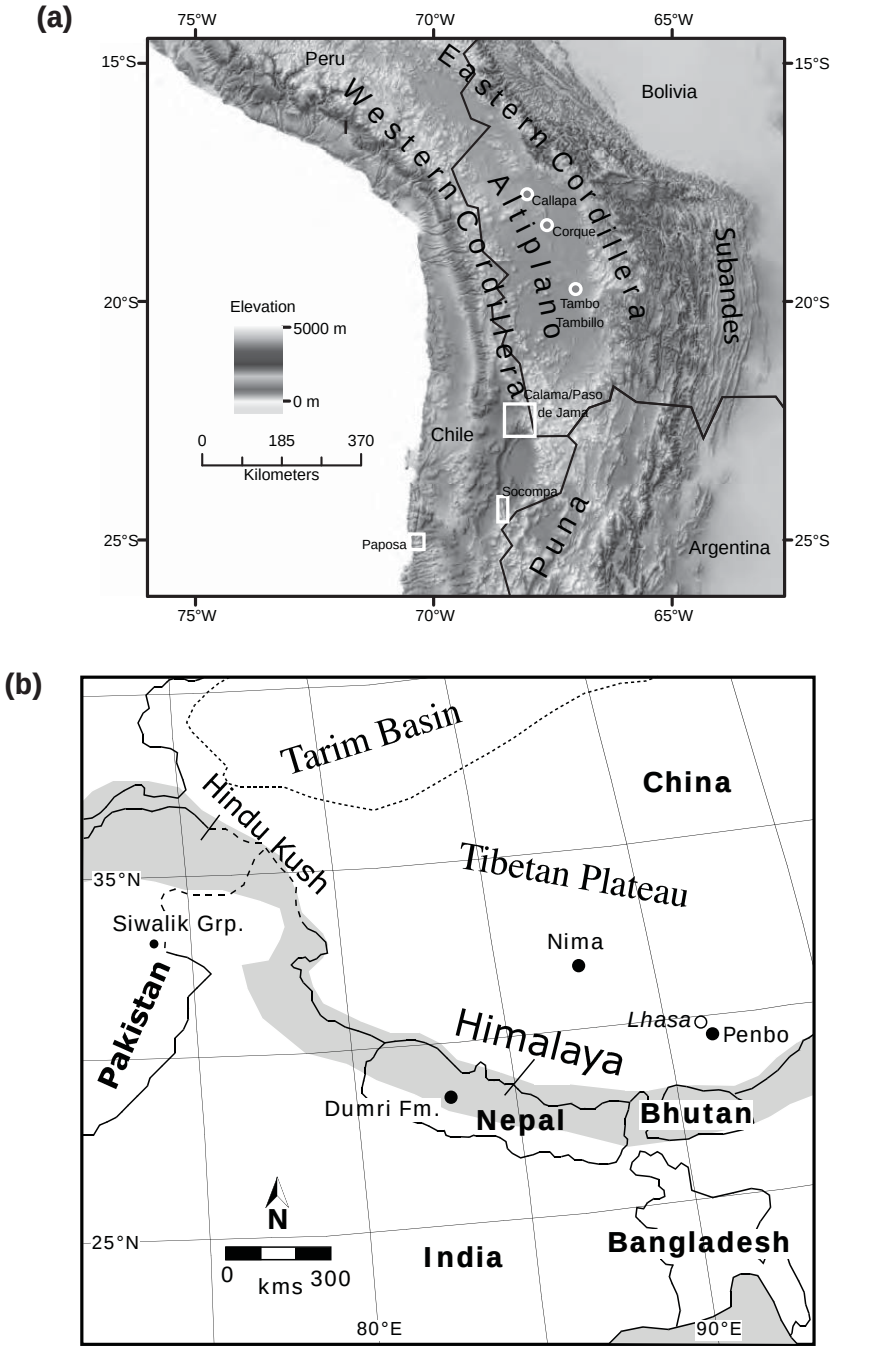

Figure 1. (a) Elevations of the Central Andean plateau between 15°S and 26°S, constructed with SRTM30 dataset. White circles show our late Oligocene to late Miocene sites discussed in the text. White boxes enclose study sites for modern soil carbonate in the Atacama Desert in Quade et al. 2007; (b) location figure for study locations in Himalayan-Tibet orogen (Himalaya/Hindu Kush shaded).

(or $\delta^{18}O_{sw}$, expressed in ‰ relative to SMOW) (Garzione et al. 2000a,b; Rowley et al. 2001; Blisniuk et al. 2005; Currie et al. 2005; Rowley and Currie 2006). The $\delta^{18}O$ value of soil water can differ from $\delta^{18}O_{mw}$ values due to evaporative enrichment of ^{18}O in soil water (Cerling and Quade 1993). Moreover, the season of carbonate precipitation may also affect the isotopic composition of pedogenic carbonate, both in terms of seasonal variability in the temperature of carbonate formation and the isotopic composition of rainfall and soil water (e.g., Quade et al 1989a; Amundson et al. 1996; Liu et al. 1996; Stern et al. 1997).

These competing effects can be mitigated by the application of a new "clumped-isotope" carbonate thermometer that allows the determination of the temperature of carbonate formation (Ghosh et al. 2006a). This technique relies on the abundance of bonds between rare, heavy isotopes (i.e., ^{13}C-^{18}O) in the carbonate mineral lattice, the relative abundance of which increases at lower temperatures. Recent paleoelevation studies (Ghosh et al. 2006b) applied this carbonate thermometer to better constrain $\delta^{18}O_{sw}$ values from which paleoelevation was calculated using the traditional approach (Garzione et al. 2006).

We will begin this review by evaluating modern variability in $\delta^{18}O$ values of surface waters with elevation change across the Andean plateau (Fig. 1a) and the Himalayan-Tibet plateau (Fig. 1b). Global patterns of the $\delta^{18}O_{mw}$/elevation relationship are comprehensively reviewed in Poage and Chamberlain (2001) and Blisniuk and Stern (2005). We will then compare $\delta^{18}O_{mw}$ to $\delta^{18}O_{sc}$ results from the Mojave Desert, the Andes, and Tibet, among the few regions where coupled water and carbonate isotopic data from modern soils are available, providing an essential interpretive backdrop for the paleosol carbonate records. Finally, we present case studies from the Andes and Himalaya-Tibet as examples of the use of $\delta^{18}O$ and "clumped-isotope" values from pedogenic carbonates in paleoelevation reconstruction.

DEPENDENCE OF THE ISOTOPIC COMPOSITION OF RAINFALL ON ELEVATION

$\delta^{18}O_{mw}$ values decrease with elevation gain on both sides of the Andes and Tibet (Fig. 2a). On the windward side, these changes reflect the expected effects of progressive distillation on air masses as they rise, cool, and rain out over an orographic barrier. Interestingly, $\delta^{18}O_{mw}$ values also decrease with elevation on the leeward sides of large mountain ranges, especially in warm climates (summarized in Blisniuk and Stern 2005), including the western flank of the central Andes, the Himalaya, and to some extent the Sierra Nevada's. This is not predicted by Rayleigh distillation models of cloud mass rain out (Rowley and Garzione 2007). Some research suggests that in dry leeward settings, raindrops are evaporatively enriched in ^{18}O during descent, and a small fraction of the original raindrop reaches the ground (Beard and Pruppacher 1971; Stewart 1975). Thus, evaporative gains in raindrop ^{18}O apparently more than offset Rayleigh-type depletions in ^{18}O in the original cloud mass.

One striking example of this pattern is from the Andes, drawing mainly upon published data between 17-21°S from Gonfiantini et al. (2001) and our unpublished water data for the eastern side of the Andes, and from Fritz (1981) and Aravena et al. (1999) for the Pacific slope (Fig. 2a). For the eastern slope, $\delta^{18}O$ values decrease by ~2.6 ‰/km across an elevation gain of 2200 m. These results match well with $\delta^{18}O$ values of snow from Mt. Sajama (Hardy et al. 2003), and rain falling on Lake Titicaca (Cross et al. 2001). On the Pacific slope, samples collected from 22 stations over a four-year period show an even steeper isotopic lapse rate of −6.2 ‰/km. We will return to these data when we look at isotopic results from modern pedogenic carbonates in this region.

Stream-water sampling from Garzione et al. (2000a) along the Kali Gandaki up the south face of the Himalaya at about 78°E shows a very regular decrease in $\delta^{18}O_{mw}$ values (Fig. 2b). The best fit to these data is a second-order polynomial, with an average decrease of around 2.5

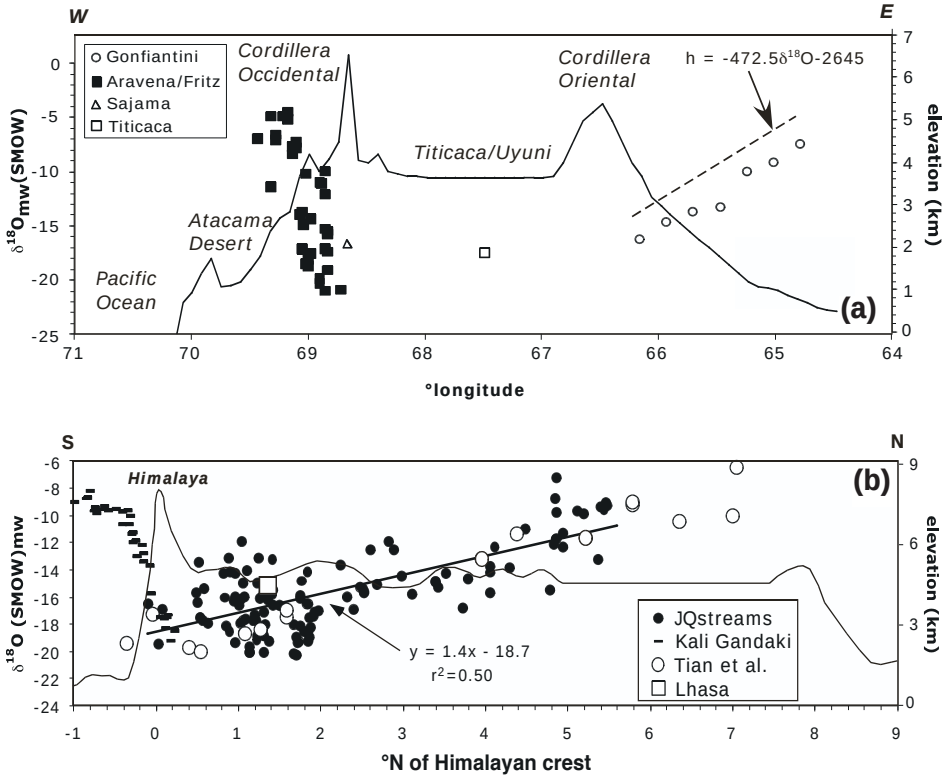

Figure 2. Topography and $\delta^{18}O_{mw}$ (SMOW) values for (a) the Andes, compiled from Aravena et al. (1999) and Fritz et al. (1981); Hardy et al. (2003) (Sajama); and Cross et al. (2001)(Titicaca); uncorrected Gonfiantini et al. (2001); dashed line and equation are corrected Gonfiantini data combined with our unpublished data (see also Fig. 14 and text); and (b) for Tibet, compiled from Garzione et al. 2000a (Kali Gandaki); Tian et al. 2001; Quade unpublished data (JQ streams); and Araguás-Araguás 1998 (Lhasa).

to 2.7 ‰/km. $\delta^{18}O_{mw}$ values decrease to below −20‰ for elevations above 5000 m, as sampled near high-elevation glaciers (Zhang et al. 2002; Tian et al. 2005) and from streams flowing from the highest elevations on both sides of the Himalaya (Tian et al. 2001). The more unexpected pattern is the increase in $\delta^{18}O_{mw}$ values north of the Himalayan crest, as observed by Tian et al. (2001) and Zhang et al. (2002). The sampling stations are widely dispersed, and we can add our own unpublished stream water samples from about 29-34°N. The combined data display an increase of ~1.5 ‰/° latitude. Virtually all the collection stations range from 3700 m to 5000 m. With our own stream-water samples, we show sampling elevations (Fig. 2b) unadjusted for the more relevant mean elevation and latitude of the catchment. But since we sampled mostly small catchments, we believe the correlation with Tian's and Zhang's data is not a coincidence.

The southwest Indian monsoon dominates rainfall south of the Himalayan front as well as stations immediately north of the crest, perhaps mixed from some contribution from the East Asian monsoon. The seasonal distribution of $\delta^{18}O_{mw}$ values for Lhasa, located 1.5° north of Himalayan ridgecrest, illustrates this. Over ninety per cent of the rain falls in the summer rainy season, and that rainfall displays much lower $\delta^{18}O_{mw}$ values than winter snow and rain (Araguás-Araguás et al. 1998). The strong ^{18}O and D depletions in summer rainfall can be modeled in terms of gradual, Rayleigh distillation of moisture (Rowley et al. 2001) that derives water vapor

from the equatorial Indian Ocean or East China Sea, is drawn northward and westward over land in the summer, and rises, cools and rains out as it passes over the Himalaya and Tibet.

This simple picture does not explain the gradual increase in $\delta^{18}O_{mw}$ values north of the Himalayan crest. Mean elevation of sampling sites north of the crest lies almost entirely within 4500 ± 500 m, and even increases slightly northward, the opposite of the expected pattern where elevation is the main determinant of $\delta^{18}O_{mw}$ values. Likewise, the continentality effect—simple rain out of air masses with distance from coastlines—should cause $\delta^{18}O_{mw}$ values to decrease inland, not decrease.

The explanation provided by Tian et al. (2001) and supported by a variety of data, including seasonality of rainfall and deuterium excess, is that other, either local or northerly derived air masses penetrate southward during the winter months. The $\delta^{18}O_{mw}$ value of stream samples and amount-weighted rainfall samples increase northwards, reflecting a decreasing proportion of summer (monsoonal) rainfall in year-round weighted rainfall. The key point for paleoelevation reconstruction is that $\delta^{18}O_{mw}$ values change quite significantly across the Tibetan Plateau for climatic, not elevational reasons. The result is that lapse rates in the southern plateau (−2.6 ‰/km) are almost twice those of the northern plateau (−1.5 ‰/km). Consequently, paleoelevation estimates depend on distance of sampling sites from the Himalayan range crest, and how climate change in the past, such as a strengthened or weakened Asian monsoon, might have increased or decreased isotopic lapse rates northward on the plateau.

MODERN PEDOGENIC CARBONATES

Pedogenic carbonate formation

The general equation for weathering (to the right) and calcite precipitation (to the left) in soils is:

$$CaCO_3(s) + CO_2\,(g) + H_2O = Ca^{++}\,(aq) + 2HCO_3^-\,(aq) \quad (1)$$

Here we use calcite as the parent material but in its place just as easily could have used Ca-Mg silicate minerals. Pedogenic carbonate formation (to the left) is driven by both soil water and CO_2 loss. Seasonality of carbonate formation is not known for certain, but in most settings it is likely concentrated in the summer half year when soils are thawed or warmer, plants are active and evapotranspiring, and evaporation is greatest.

In well-drained soil profiles, water for weathering reactions like (1) is supplied directly by local rainfall. Pedogenic carbonate thus enjoys a key advantage over other types of carbonate in paleoelevation reconstruction in that it forms from rainfall that fell on the site, and not runoff from higher elevations, as in the case of many riverine and lacustrine carbonates. For the oxygen system, molar water to rock ratios are extremely high in soils, and thus the $\delta^{18}O$ value of secondary weathering phases such as clays, iron oxides, and carbonates should not be influenced by parent material during weathering. Analogously, for the carbon system in most soils, the molar $C_{plant}/C_{parent\ material}$ is also very large, and hence plant CO_2 mixed with the atmospheric CO_2, and not carbon from local parent material such as limestone, will determine the $\delta^{13}C$ value of pedogenic carbonate. In dry climates, soils dewater largely by a combination of evapotranspiration (ET) and evaporation (E), with some percolation through to the local water table. The ratio of dewatering by these processes (F_E/F_{ET}) decreases with increasing soil depth and increasing rainfall. For oxygen isotopes in soils, evaporation is a fractionating process, enriching residual soil water in ^{18}O. By contrast, evapotranspiration is a non-fractionating process; water is drawn unfractionated into plant roots from the soil. Hence, in drier climates and shallower in soils, evaporative enrichment in ^{18}O has been widely observed (e.g., Allison et al. 1983; Hsieh et al. 1998). After correction for temperature (discussed later), this effect should also be expressed in secondary mineral phases, such as carbonates in soils.

In the next section we compare $\delta^{18}O_{sc}$ values to local $\delta^{18}O_{mw}$ values from rainfall collected sometime in the last few decades. To make this comparison, we use pedogenic carbonate samples that formed recently, preferably over the latter part of the Holocene, on the assumption that this is the carbonate most likely to represent isotopic equilibrium conditions between calcite and the sampled water. In the absence of radiometric dates from our samples, we use pedogenic carbonate morphology as a qualitative indicator of age, following the conventions of Gile et al. (1966) (see also Machette 1985), in which thin carbonate coatings on alluvial clasts represent Holocene-age cements, and continuous filling of the soil matrix by carbonates represents older (10^4-10^6 yrs) Quaternary cementation.

The oxygen isotopic composition of Holocene pedogenic carbonate

Salomans et al. (1978), Talma and Netterberg (1983) and Cerling (1984) were among the first to show that $\delta^{18}O_{mw}$ values are positively correlated with the $\delta^{18}O_{sc}$ values, a relationship later shown to hold true for a variety of meteoric cements (Hays and Grossman 1991). The details of this relationship are worth exploring in light of newer data and from the perspective of paleoelevation reconstruction. To do this we selected three data sets that encompass the broad range of rainfall (~20 to 1000 mm/yr) in which pedogenic carbonates develop. These include modern pedogenic carbonates from the relatively wet mid-western USA (Cerling and Quade 1993), the Mojave Desert (Quade et al. 1989a), and from the extremely arid Atacama Desert (Fig. 1a; Quade et al. 2007). We compare $\delta^{18}O_{sc}$ values from Holocene-age soils against predicted $\delta^{18}O_{sc}$ based on local mean annual temperature (MAT) + 2 °C (see defense of this formulation in the next section of the paper) and known $\delta^{18}O_{mw}$ values (Fig. 3). In higher rainfall areas, predicted and observed $\delta^{18}O_{sc}$ values are positively correlated, as observed by others previously (i.e., Salomans et al 1978; Cerling 1984). The departures of observed $\delta^{18}O_{sc}$ values from the 1:1 predicted line are larger where the climate is drier, consistent with evidence from modern soil water studies (e.g., Hsieh et al. 1998). Hence, pedogenic carbonates from the driest sites in the Mojave (MAP < 100 mm/yr) and in nearly all sites in the hyperarid Atacama Desert

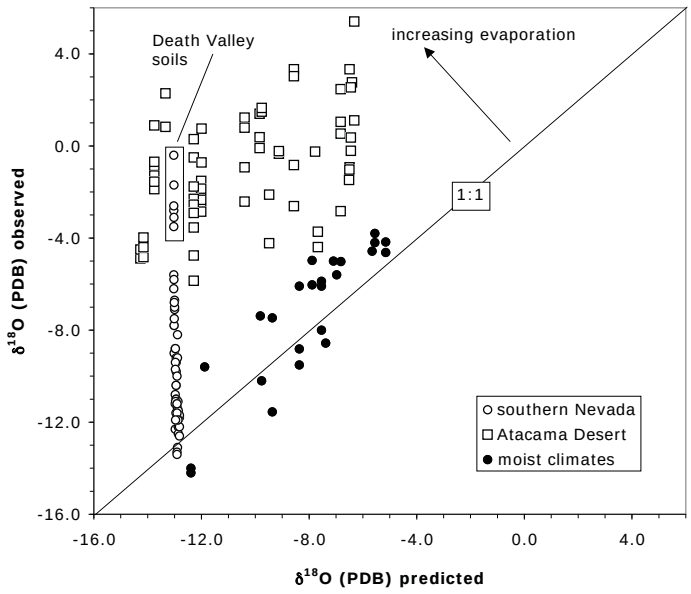

Figure 3. Observed $\delta^{18}O_{sc}$ (data from Quade et al. (1989a) and Cerling and Quade (1993), and Quade et al. (2007)) versus predicted $\delta^{18}O_{sc}$ values based on local mean annual temperature and $\delta^{18}O_{mw}$ values.

(2-114 mm/yr) show the strongest soil evaporation effects. Examination of $\delta^{18}O_{sc}$ values collected with depth in soil profiles is also instructive. In dry settings like the Mojave Desert, $\delta^{18}O_{sc}$ values increase toward the surface (Fig. 4), whereas from moister settings like Kansas, $\delta^{18}O_{sc}$ values show little variation with soil depth (Cerling and Quade 1993).

In the context of paleo-elevation reconstruction, the following conclusions can be drawn: (1) in moister climates, $\delta^{18}O_{sc}$ values should provide a close approximation of $\delta^{18}O_{mw}$ values after correction for temperature, (2) in drier settings, $\delta^{18}O_{sc}$ values will be influenced by evaporative enrichment, and hence in this instance (3) sampling laterally and deeper (≥ 50 cm) in soils should produce a better approximation of unevaporated $\delta^{18}O_{mw}$ values. Because of evaporation effects, $\delta^{18}O_{sc}$ values should be viewed to provide only maximum estimates of $\delta^{18}O_{mw}$ values and thus minimum estimates of paleo-elevation.

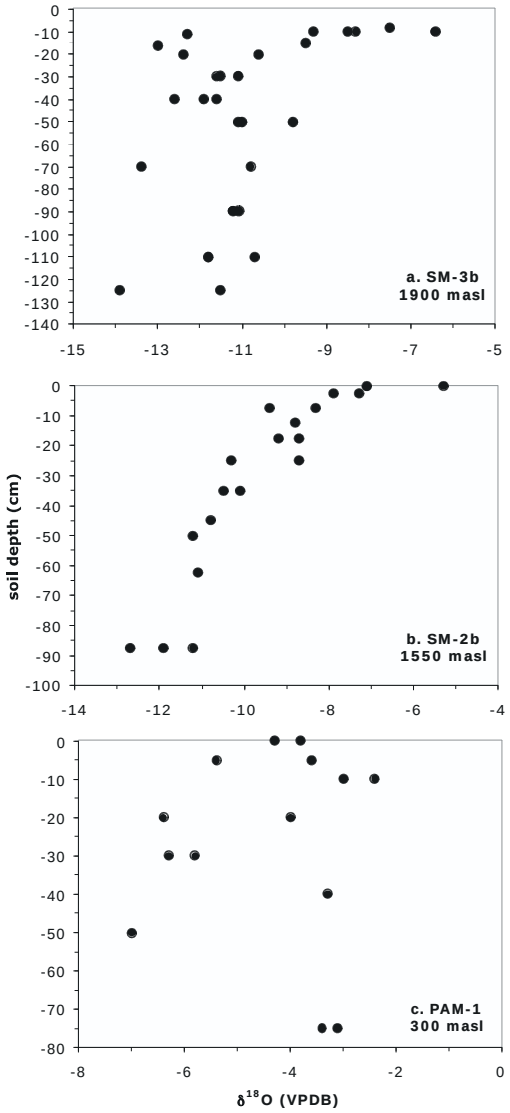

Figure 4. Depth profiles of $\delta^{18}O_{sc}$ (PDB) versus soil depth, from three sites in the Mojave Desert, (a) SM-3 (1990 masl), (b) SM-2b (1550 masl), and (c) PaM-1 (300 masl), all from Quade et al. (1989a).

Soil temperature considerations

One must be able to constrain soil temperature (*T*) to account for the fractionation between calcite and water. In this regard, several factors favor the use of pedogenic carbonates. One is that the fractionation factor between calcite and water is *T* small (~ −0.22 to −0.24 ‰/°C in the range 0-30 °C) when compared, for example, to the steep average dependence of $\delta^{18}O_{mw}$ values on elevation of −2.8 ‰/km. Thus, $\delta^{18}O_{sc}$ values are widely used by geologists to constrain $\delta^{18}O_{mw}$ values, as in paleo-elevation reconstructions, but only used for paleo-temperature reconstructions in a narrow set of circumstances where paleo-$\delta^{18}O_{mw}$ values are relatively invariant. Having said this, the effects on $\delta^{18}O_{sc}$ values of decreasing *T* with elevation can partially to entirely offset the influence of decreases in $\delta^{18}O_{mw}$ values with elevation. Temperature lapse rates globally are about 5-6°C/km. This temperature lapse rate combined with a −2.8 ‰/km decrease in $\delta^{18}O_{mw}$ values would produce a ca. −1.5 ‰/km change with elevation gain in $\delta^{18}O_{sc}$ values.

One feature of soils that confers a significant advantage compared to other carbonates (such as lacustrine carbonate) is that soil T converges toward mean annual air *T* at depth. In contrast, shallow aquatic systems where many carbonates form can experience sharp diurnal and seasonal changes. Soil *T* varies with time (*t*) and exponentially as function soil depth (*z*) following (from Hillel 1982):

$$T(z,t) = T_{avg} + A_{\circ}\left[\sin\left(\omega t - z/d\right)\right]/e^{-z/d}$$

where T_{avg} is average air temperature, A_o is seasonal or diurnal maximum and minimum *T* amplitude at $z = 0$, ω is radial frequency, *z* is soil depth, *d* is the "damping" depth (or 1/*e* folding depth) characteristic of the soil:

$$d = \left(2\kappa/C_V\omega\right)^{1/2} \quad (2)$$

where κ is thermal conductivity and C_V is volumetric heat capacity. As regards surface-*T* fluctuations, the 1/*e* folding depth of diurnal fluctuations in the order of centimeters, much shallower than the average depth of carbonate accumulation. This is due mainly to the high diurnal radial frequency (in which $\omega = 2\pi/86{,}400$ seconds), which in Equation (2) is inversely related to the damping depth. Seasonal temperature fluctuations have a much lower radial frequency, hence greater damping depth. Therefore, it is seasonal fluctuations in *T*, and their attenuation at deep soil depths (> −20 cm) where soil carbonate forms, that is the chief concern here.

Taking the hypothetical example of a Tibetan soil near Lhasa at 4100 m, we assume in the following simulation 0.0007 cal/cm sec, and 0.3 cal/cm^3 °C for κ and C_V (from Hillel 1982), respectively. This yields 1/*e* folding lengths for seasonal temperature change of plateau soils of about 150 cm.

Average ground temperature differs by 1-3 °C from average air temperature due to excess ground warming during the summer months (Bartlett et al. 2006). This offset is correlated with mean radiation received at a site (1.21 K/100 W m^{-2}), which is in turn is a function of vegetation cover, slope aspect, and latitude. For our calculations we added a constant 2 ± 1 °C to average air temperature to arrive at average ground temperature at depth.

Depth of pedogenic carbonate formation is typically between 50 and 150 cm on the Tibetan plateau. At these high elevations the soil is at or below freezing half of the year. Thus we can assume that pedogenic carbonate formation occurs during the summer half year, when soils thaw or are warmer, evaporation is greatest, and when plants are actively transpiring soil water. For our Tibetan soil site at 4100 m, monthly mean extremes in air temperature range between 11.6 and −6.4 °C, around a mean of about 2.6 °C. This yields a modeled seasonal T amplitude of about 12.7 °C at 50 cm to 6.7 °C at 150 cm (**Fig. 5**). For the summer half-year, this produces a range of 1.5 to 0.7‰ uncertainty in the estimation of paleo-$\delta^{18}O_{mw}$ from pedogenic carbonate sampled from 50 to 150 cm soil depth, respectively (Fig. 5b). Here we use the fractionation factor (α) between calcite and water of $1000\ln\alpha_{calcite\text{-}water} = (18030/T) - 32.42$, where *T* is in Kelvins (Kim and O'Neil 1997). We can conclude that deeper sampling is better for reducing the error in paleo-elevation reconstruction arising from seasonal fluctuations in temperature. The contribution to the error can be no less than on the order ~0.8‰ for typical Tibetan soils; in other words, about 300 m in paleoelevation terms.

Evaluation of aridity

Aridity is of interest in paleoelevation reconstruction for two reasons: (1) in extreme aridity cases, the $\delta^{18}O_{sc}$ values are dominated by evaporation, and realistic estimates of paleoelevation are probably not obtainable, no matter the sampling density, and (2) aridity develops in rain shadows, and thus may provide qualitative evidence of orogenic blockage of moisture.

Evaluation of paleoaridity can (and should) be approached both qualitatively and quanti-

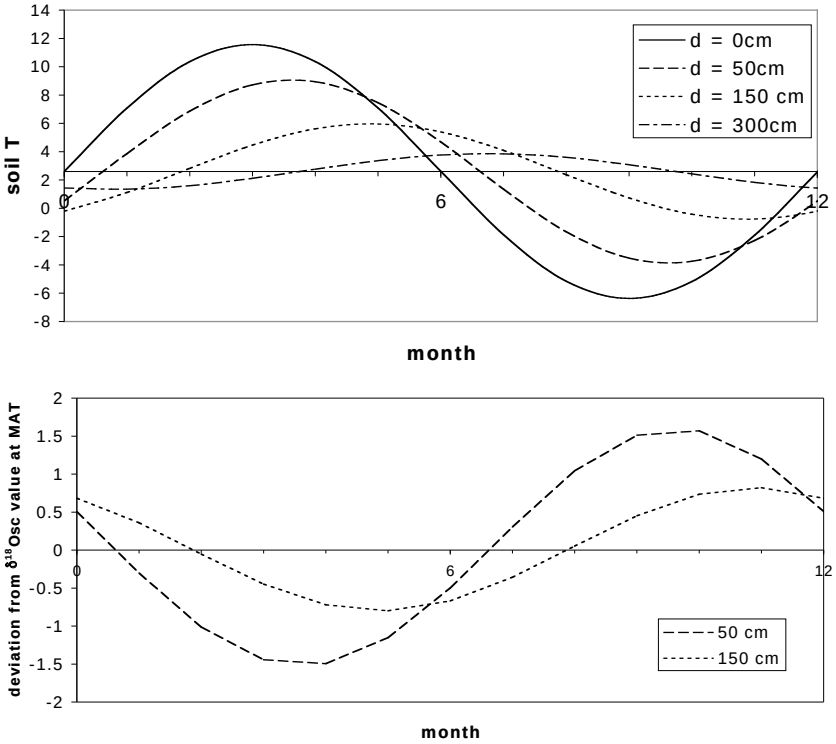

Figure 5. Depth profiles of soil temperature for a site at 4100 m in southern Tibet (see text) calculated using MAT from nearby Lhasa (3660 m) of 8°C and a local air-*T* lapse rate of 6 °C/km, a) showing modeled seasonal fluctuations in soil temperature at various depths, and (b) seasonal deviations from predicted $\delta^{18}O_{sc}$ values at MAT.

tatively. The qualitative approach involves both soil morphology and carbonate leaching depth. Rech et al (2006) provides one recent example from the central Atacama Desert of the utility of paleosols in establishing the limits on paleo-aridity (Fig. 1a). They showed that hyperarid (< 20 mm/yr) conditions have prevailed—based on the presence of buried nitrate and gypsic paleosols—in the central Atacama Desert since at least 12 Ma. In this setting where evaporation strongly distorts $\delta^{18}O_{sc}$ values, useful estimates of paleo-elevation are hard to obtain, as we will argue in a later section of the paper. Rech et al (2006) go on to describe older calcareous paleosols in the ~20 Ma range characterized by strong reddening, visible secondary clay accumulations, and vertic fracturing of the paleosol. These are all features uncharacteristic of calcareous paleosols of the current Atacama Desert, and a good match to modern soils now found in moister central Chile where mean annual rainfall (MAP) is > 200 mm/yr. These kinds of pedogenic carbonates are much better targets for paleoelevation reconstruction.

In addition to reddening and clay content (Birkeland 1984), depth of pedogenic carbonate leaching is a useful qualitative index of paleoaridity. In modern soils, leaching depth increases by 0.2 to 0.3 cm/cm rainfall (Jenny and Leonard 1934; Royer 1999; Wynn 2004). The scatter around this relationship is very large, due to a host of factors such as erosion of paleosol surfaces, texture of parent material, local drainage conditions, and so forth (Royer 1999). In our experience, depth of leaching is useful where multiple paleosols can be observed, vertically and along strike, in an attempt to average out some of the non-climatic influences listed above.

For a more quantitative approach to paleoaridity, carbon isotopes from pedogenic carbonate can provide evidence of soil respiration rates, which are closely related to plant cover at a site, and hence aridity. Respiration rates cannot be calculated from $\delta^{13}C_{sc}$ values without independent knowledge of $\delta^{13}C$ values of local plant cover, because both C_3 and C_4 plants compose modern vegetation. C_4 plants expanded across low-latitude and mid-latitude ecosystems between 8 and 4 Ma, prior to which time C_3 plants appear to dominate most ecosystems (Cerling et al. 1997; but see also Fox and Koch 2004). This ecologic simplification makes estimation of paleo-respiration rates from $\delta^{13}C_{sc}$ values possible prior to about 8 Ma, since the only two end members contributing to soil CO_2 are C_3 plants and the atmosphere (Fig. 6). Prior to the mid-Oligocene, pCO_2 appears to have been much higher (Pagani et al. 1999; Pearson and Palmer 2000; Pagani et al. 2005), once again complicating estimation of paleo-respiration rates. But for the period 30-8 Ma, paleo-respiration rates can be calculated from $\delta^{13}C_{sc}$ values alone, allowing us to trace the development of rain shadows in the lee of both the emerging Himalaya and Andes.

The basic principle, first modeled in Cerling (1984) and modified in Davidson (1995) and Quade et al. (2007), is that the $\delta^{13}C$ value of soil CO_2, and the pedogenic carbonate from which it forms, is determined by the local mixture of C_3 plant CO_2 and atmospheric CO_2. In general, the deeper in the soil profile or the higher the soil respiration rate, the greater the influence of plant-derived CO_2. Thus, for a given soil depth, $\delta^{13}C_{sc}$ values are determined by soil respiration rate. Temperature has a very modest effect on carbon isotope fractionation (~ –0.11 ‰/°C). As an example, $\delta^{13}C_{sc}$ values will increase from –4.6 to –9.4‰ as respiration rates increase from 0.5 to 8 mmoles/m^2/hr at 9 °C (Fig. 6), where > 0.5 mmoles/m^2/hr roughly translates into MAP > 200 mm/yr in the Mojave Desert. Later in the paper we will use this framework to interpret $\delta^{13}C_{sc}$ values from Tertiary-age carbonates in Himalaya/Tibet and the Andes.

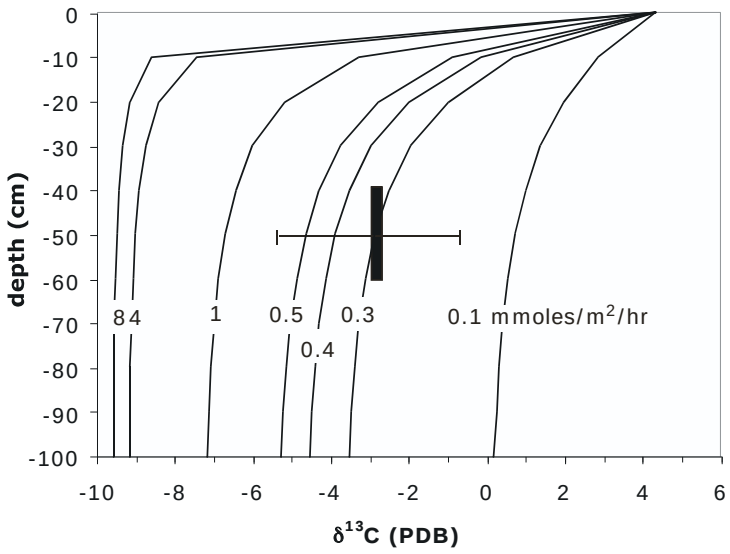

Figure 6. Changes in the $\delta^{13}C$ (PDB) value of soil carbonate at various respiration rates (indicated) in a pure C_3 world and at low pCO_2 (400 ppmV) from 30 to 8 Ma, as predicted by the one-dimensional diffusion model of Cerling (1984) and Quade et al. (2007), assuming $\delta^{13}C$ (PDB) of plants = –25‰, $\delta^{13}C$ (PDB) of the atmosphere = –6.5‰, an exponential form to CO_2 production with depth, and characteristic CO_2 production depth (k) of 32 cm. Black bar denotes range of sampled carbonate soil depths and average $\delta^{13}C_{sc}$ (PDB) values from late Oligocene paleosol carbonate samples from Nima, southern Tibet; horizontal error bar reflects uncertainties in soil porosity = 0.5 ± 0.1 (see Hillel 1982), T = 9±3°C, and pCO_2 = 400 ± 100 ppmV (see Pagani et al. 2005).

Elevation variation in the $\delta^{18}O_{sc}$ value of pedogenic carbonate

It follows from our previous discussion of modern pedogenic carbonates that there should be a strong correlation between elevation of sites and local $\delta^{18}O_{mw}$, and hence $\delta^{18}O_{sc}$ values. For all the interest in paleoelevation reconstruction, there is surprisingly little ground-truthing of the elevation-$\delta^{18}O_{sc}$ relationship by direct sampling of modern carbonates. Most studies simply calculate theoretical $\delta^{18}O_{sc}$ values using some assumed $\delta^{18}O_{mw}$/elevation relationship, and local MAT. Here we explore the validity of these assumptions by looking at actual, not theoretical, $\delta^{18}O_{sc}$ values from modern soils from different elevations in southern Nevada, Tibet, and the Pacific slope of the Andes. Our conclusion is that $\delta^{18}O_{sc}$ values from the warm and arid Mojave and hyperarid Atacama are severely affected by evaporation, whereas evaporation effects are much reduced in carbonates from moist India/Nepal and dry but very cold Tibet.

$\delta^{18}O$ values of modern (= Holocene) pedogenic carbonate collected from 50 cm depth in Death Valley and up the east faces of the Spring and Grapevine Mountains of southern Nevada decreases steeply with elevation gain by about −5.5 ‰/km (r^2 = 0.65) (Quade et al. 1989a) (**Fig. 7**). By comparison, the $\delta^{18}O_{mw}$ values compiled from 32 stations located across the region decreases with elevation by a modest 1.3 ‰/km (r^2 = 0.4) (Friedman et al. 1992). If these $\delta^{18}O_{mw}$ values are representative of rainfall falling on soil sites, the $\delta^{18}O_{sc}$ values predicted to form in equilibrium with them (adjusting for temperatures at each site) would all be around −13‰ (Fig. 7), and virtually invariant with elevation. We only observe these very low values deep in soils at the wetter sites (MAP > 200 mm/yr). The residual between observed and predicted $\delta^{18}O_{sc}$ values is strongly correlated (**Fig. 8**; r^2 =0.76) with mean annual rainfall. This shows that almost all of the steep gradient in $\delta^{18}O_{sc}$ values that we observe over a 3000 m elevation range

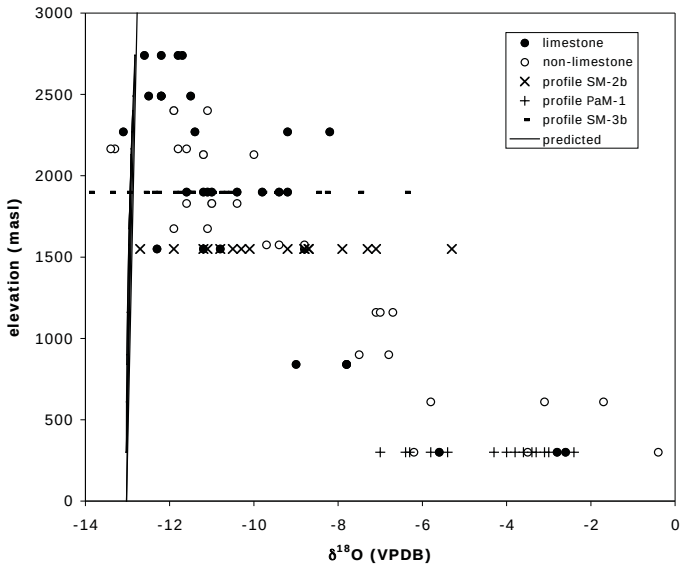

Figure 7. $\delta^{18}O_{sc}$ (PDB) of soil carbonate collected from ~50 cm soil depth versus elevation (masl) from Holocene-age soils in the Mojave Desert (from Quade et al. 1989a). Soil carbonate collected on both limestone and non-limestone parent materials show the same approximate decrease with elevation of −5.5 ‰/km. Soil profile values are the same as in Figure 4. The line denotes the $\delta^{18}O_{sc}$ (PDB) predicted from local $\delta^{18}O_{mw}$ values from 33 rainfall collection sites in the Mojave Desert ($\delta^{18}O_{mw}$ (SMOW) = −0.0013 × elevation (m) − 10.68; r^2 = 0.39; converted from δD values using $\delta D = 7.2\delta^{18}O + 7.8$) compiled from Friedman et al. (1992), using MAT + 2 °C at each site (T (°C) = −0.0079 × elevation (m) − 23.07; r^2 = 0.93; 8 climate stations).

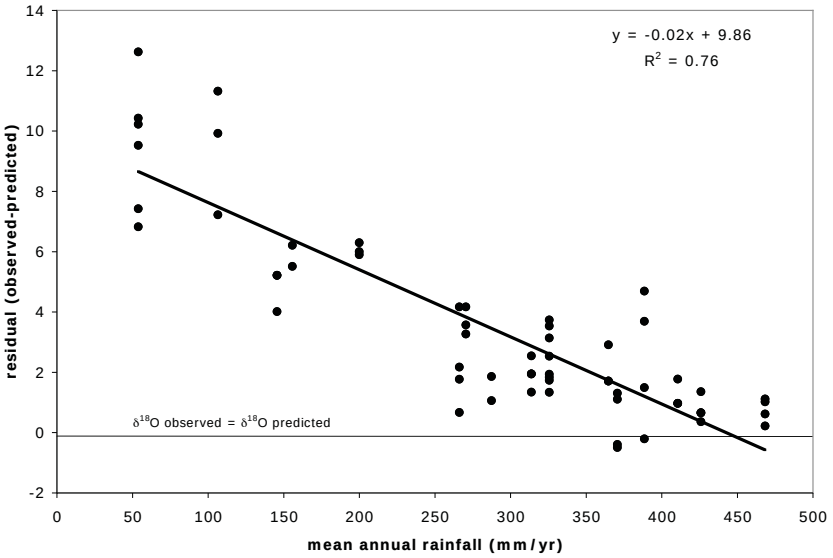

Figure 8. The residuals calculated from Figure 7 plotted against mean annual rainfall for each Mojave Desert site.

is produced by evaporation, and changes in $\delta^{18}O_{mw}$ values have little influence. At rainfall rates below 200 mm/yr, $\delta^{18}O_{sc}$ values from the same pedogenic carbonates are highly enriched in ^{18}O by evaporation (Fig. 8), and can yield large (> 2 km) underestimates of actual elevation.

We recently completed a transect up the Pacific slope of the Andes at 24°S (Fig. 1a; **Fig. 9**). The transect spans the central sector of the Atacama Desert, one of the driest regions in the world. $\delta^{18}O_{sc}$ values for samples > 50 cm depth from this transect vary between −5.9 and +5.4‰. Scatter of data within one profile or across several profiles in a narrow elevation range is very large, often > 5‰, even from samples deeper than 50 cm. In spite of this scatter, the most negative $\delta^{18}O_{sc}$ values decrease modestly with elevation, from as low as −2‰ on the coast to −5.9‰ at 3400 m, with an excursion toward higher values in the driest part of the transect between about 1000 and 2500 m, a region so dry that it is virtually plantless.

The $\delta^{18}O_{mw}$ values from Fritz (1981) and Aravena et al. (1999) can be used to predict $\delta^{18}O_{sc}$ values assuming MAT + 2 °C at soil depth, with an error of ≤ 1.5‰ at ≥ 50 cm, as calculated in a previous section. In the coastal Atacama, fog drip outstrips rainfall from the rare Pacific storm (Larrain et al. 2002), and hence we compare $\delta^{18}O_{mw}$ values of fog (Aravena et al. 1989) and of local rainfall as assumed parent waters in the coastal zone. We find that observed $\delta^{18}O_{sc}$ values always exceed predicted $\delta^{18}O_{mw}$ values (Fig. 9). Predicted $\delta^{18}O_{sc}$ values along the transect between sea level and 4000 m are between about −3 and −15‰, whereas the *most negative* observed $\delta^{18}O_{sc}$ values range between −3 and −5.9‰. Clearly, the prognosis for meaningful paleoelevation reconstruction in such arid conditions is poor. For example, even with our very large sample size of >60 from between 3000 and 4000 m, we would underestimate paleoelevation using only the most negative values by at least 1 km. This is why it is vital to make some assessment of paleoaridity independent of the conventional $\delta^{18}O_{sc}$ measurements.

The second data set that we briefly consider comes from selected locations along a north-south transect across the Himalaya and Tibet (**Fig. 10**). This is work in progress, but enough information is already in place to make some useful observations. As with other data sets, we focused on sampling deeper (> 50 cm) carbonate from younger profiles, although in the case of

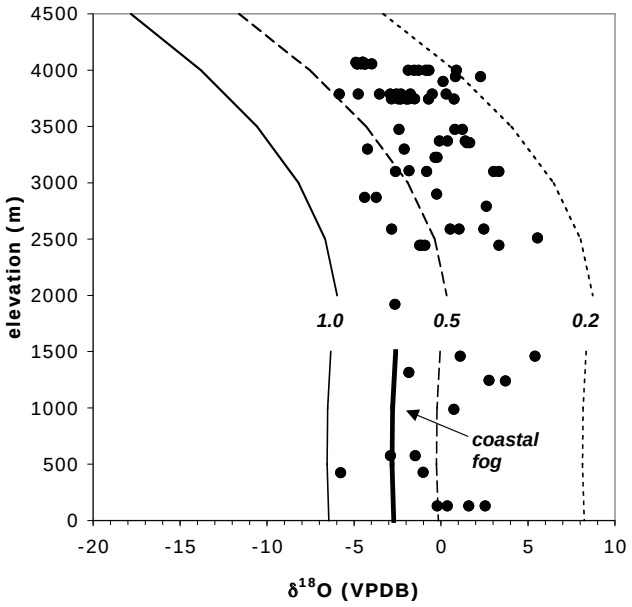

Figure 9. $\delta^{18}O_{sc}$ (PDB) values of Holocene soils versus elevation in the Atacama Desert, between 22.5 and 25°S. The thin lines (solid, dashed, dotted) denote modeled fraction (f) of soil water remaining after evaporation, using local site MAT and $\delta^{18}O_{mw}$ (SMOW) values for rainwater (from Aravena et al. 1999 and Fritz 1981); and the thick line for f = 1.0 for coastal fog from Aravena et al. (1989).

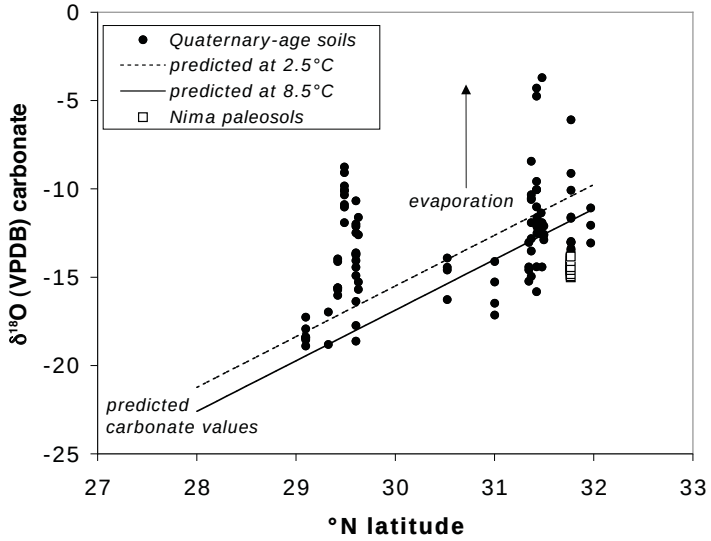

Figure 10. $\delta^{18}O_{sc}$ (PDB) values from Quaternary-age soils across the Himalayan-Tibetan orogen, and "corrected" values (see text) from late Oligocene paleosols at Nima. Lines denote $\delta^{18}O_{sc}$ (PDB) values predicted at a range of soil temperatures (indicated), and using the regression equation of unpublished water data across the Tibetan plateau shown in Figure 2b.

Tibet we also obtained carbonates from older geomorphic surfaces, in order to develop some perspective on the isotopic effects of climate variability during the Quaternary.

In general, $\delta^{18}O_{sc}$ values follow the expected pattern based on changes in modern $\delta^{18}O_{mw}$ values across the Himalayan-Tibetan orogen (Fig. 10). To make this comparison we drew on our published and unpublished data on Holocene-age carbonates from three areas: modern Pakistan, southern Tibet, and a few scattered sites in NE Tibet. In Pakistan, twelve analyses of modern pedogenic carbonates from three profiles yield an average value of −6.3‰ (Quade and Cerling 1995). This value is very similar to the long-term average for the Quaternary-age paleosols from Pakistan (−6.4‰) and from central Nepal (−7.0) (Quade et al. 1995b). The most negative modern $\delta^{18}O_{sc}$ values of −7.7‰ in Pakistan, and −8.5‰ for the late Neogene Siwalik paleosols are also very similar, and are close to that predicted (−8.7‰) to form from weighted modern $\delta^{18}O_{mw}$ values from New Delhi (Araguás-Araguás et al. 1998). So, based on this admittedly restricted sample of carbonates and rainfall, the system appears to be well-behaved: we can accurately reconstruct paleo-elevation for these sites during the late Neogene, which have always been at low elevation (< 500 m), using the most negative $\delta^{18}O_{sc}$ values, and the scatter of $\delta^{18}O_{sc}$ values is relatively low (< 3‰), indicating only modest evaporative modification.

Turning briefly to southern Tibet, we have preliminary data from sixteen surface soils collected between 29 and 32°N, 79 to 92°E, and 3800-5400 m. Pedogenic carbonate from these surface soils displays a range of morphologies from thin gravel coatings to pervasive matrix cements, suggestive in some cases of ages >Holocene, unlike our Mojave and Atacama soils, which are all very young (Holocene). The Tibetan samples yield a wide range of results, from −18 to +3‰ (Fig. 10). For comparison, we can predict $\delta^{18}O_{sc}$ values using $\delta^{18}O_{mw}$ values from Figure 2b and assuming local the range of MAT + 2 °C encompassing these sites. As with the Mojave and Atacama Desert samples, many observed $\delta^{18}O_{sc}$ values exceed predicted values, again because of evaporation. Interestingly, in many cases the observed $\delta^{18}O_{sc}$ values are 1 to 5‰ more negative than expected $\delta^{18}O_{sc}$ values. Detailed consideration of this interesting but incomplete data set is beyond the scope of this review, but we believe that it may illustrate the effects of perhaps the largest uncertainty in all paleo-elevation analysis using $\delta^{18}O_{sc}$ values, that of changing climate. We suggest that modern meteoric waters probably have higher $\delta^{18}O$ values than average longer-term waters as archived by Quaternary-age pedogenic carbonates. This may be due to cyclical changes during the Quaternary in the average penetration northward of Asian monsoon rainfall into southern Tibet. If true, this would lead to overestimates of paleoelevation using modern $\delta^{18}O_{mw}$-elevation relationships. Our analyses illustrate the key advantage of sampling Quaternary pedogenic carbonates as opposed to just modern meteoric waters in calibration studies. Carbonates provide more time-depth and will tend to average out the swings in Quaternary climate.

A few samples of pedogenic carbonate from 3000-3500 m in northeast Tibet fall between −11 and −4‰ in $\delta^{18}O_{sc}$ (PDB), more positive than values in southern Tibet at comparable elevations, and consistent with overall regional trends of increasing $\delta^{18}O_{mw}$ values with latitude. $\delta^{18}O$ values of surface waters from this area and approximate elevation (Garzione et al. 2004) range from −11 to −8‰, consistent with the higher observed $\delta^{18}O_{sc}$ values.

PALEO-ELEVATION ESTIMATES USING CARBONATE "CLUMPED ISOTOPE" PALEOTHERMOMETRY

Up to this point our review has focused on reconstruction of paleoelevation using $\delta^{18}O_{sc}$ values. This approach has the advantage that suitable samples are common constituents of paleosols, the necessary analytical methods are widely available and straightforward, and the various complicating factors, such as soil-water evaporation and post-depositional diagenesis, have been studied in samples with relatively well-understood histories. Nevertheless, the

validity of this "conventional" method ultimately rests on the ability to: (1) account for the effect of temperature on the isotopic fractionation between soil water and pedogenic carbonate; and (2) distinguish orographic effects on the isotopic composition of meteoric water from other possible influences, such as seasonality, and climate and latitude change.

Ghosh et al. (2006b) present an innovation to paleoelevation reconstruction using pedogenic carbonate that potentially addresses these issues. The Ghosh et al. approach uses carbonate "clumped isotope" thermometry (Ghosh et al. 2006a; Schauble et al. 2006) to impose an independent constraint on the temperatures of pedogenic carbonate growth. This information permits a more robust estimate of the $\delta^{18}O_{mw}$ from which carbonate grew and provides an independent constraint on paleoelevation by comparison with the altitudinal gradient in surface temperature.

Principles, methods and instrumentation

Carbonate clumped isotope thermometry is based on the temperature dependence of the abundances of bonds between ^{13}C and ^{18}O in carbonate minerals. This temperature sensitivity stems from the fact that isotope exchange reactions such as:

$$Ca^{13}C^{16}O_3 + Ca^{12}C^{18}O^{16}O_2 = Ca^{13}C^{18}O^{16}O_2 + Ca^{12}C^{16}O_3 \quad (3)$$

are driven to the right with decreasing temperature. That is, ordering, or "clumping," of heavy isotopes into bonds with each other is favored at low temperatures.

We are aware of no analytical method for directly measuring the abundances of reactant and product species in equation (3) with precision sufficient for useful geothermometry. Therefore, the carbonate clumped isotope thermometer uses the abundances of analogous species in CO_2 produced by phosphoric acid digestion of carbonate (i.e., $^{13}C^{16}O_2$, $^{12}C^{18}O^{16}O$, $^{13}C^{18}O^{16}O$ and $^{12}C^{16}O_2$). These measurements are made using a gas-source isotope ratio mass spectrometer that has had its collection array modified to permit simultaneous collection of all cardinal masses 44 through 49 corresponding to CO_2 isotopologues.

Ion corrections, standardization and nomenclature for analyses of $^{13}C^{16}O_2$, $^{12}C^{18}O^{16}O$, and $^{12}C^{16}O_2$ follow established conventions (Santrock et al. 1985; Allison et al. 1995; Gonfiantini et al. 1995). $^{13}C^{18}O^{16}O$ is a special case in several respects (Eiler and Schauble 2004; Wang et al. 2004; Affek and Eiler 2006): most of the variations in its abundance in natural CO_2 (including that produced by acid digestion of naturally occurring carbonates) arise from variations in bulk isotopic composition. In other words, if a population of CO_2 molecules contains an unusually large amount of ^{13}C and/or ^{18}O, then it will contain an unusually large number of $^{13}C^{18}O^{16}O$ molecules simply because the probability of a molecule incorporating both rare isotopes is relatively high. This cause of variations in $^{13}C^{18}O^{16}O$ abundance is relatively uninteresting because it tells nothing beyond what is known from measuring $\delta^{13}C$ and $\delta^{18}O$. Therefore, the nomenclature for reporting analyses of $^{13}C^{18}O^{16}O$ considers its enrichment or depletion relative to the amount that would be present in the analyzed population of molecules if that population had a "stochastic distribution" of isotopes among all possible isotopologues; that is, if the probability that a molecule contains a given isotope in a given location within the molecule were entirely random. This enrichment or depletion is reported using values of "Δ_{47}," which are defined as the difference, in per mil, of the ratio of mass 47 to mass 44 isotopologues in a sample from that ratio expected for a stochastic distribution of isotopes in that sample. Note that the population of mass 47 isotopologues includes contributions from $^{12}C^{17}O^{18}O$ and $^{13}C^{17}O_2$, which cannot be mass discriminated from $^{13}C^{18}O^{16}O$ using existing gas source isotope ratio mass spectrometers. These species must be accounted for when calculating the expected stochastic distribution and when interpreting observed values of Δ_{47}, but are not a significant complicating factor for most materials of interest to the present discussion. Standardization of Δ_{47} values requires comparison of samples with materials that are known to have a stochastic distribution. This is generally accomplished by comparison with gases that have been internally equilibrated by heating to 1000 °C.

The relationship between growth temperature of a carbonate mineral and the Δ_{47} value of CO_2 produced by acid digestion of that carbonate is known for a variety of natural and synthetic materials (including recent pedogenic carbonate) (Fig. 11). The temperature dependence of –0.005‰ per °C is clear but subtle. Moreover, $^{13}C^{18}O^{16}O$ is an exceedingly rare isotopic species, only ~45 ppm of most natural CO_2. These factors give rise to the two principal technical limitations to carbonate clumped isotope thermometry: (1) exceptionally long analyses of ~one hour and large samples of ~5 mg are required to generate measurements of Δ_{47} having precision good enough for many problems in paleothermometry; and, (2) samples must be thoroughly cleaned by cryogenic, gas chromatographic and other procedures prior to analysis (Eiler and Schauble 2004; Affek and Eiler 2006; Ghosh et al. 2006a). The primary effect of these limitations is to slow the rate at which usefully precise measurements can be made. Previous experience suggests that the highest precision that can be consistently achieved is ~ 0.005 to 0.010 ‰ (Came et al. in review), and involves such a high level of replicate measurements and standardization that only two or three unknowns per day can be analyzed.

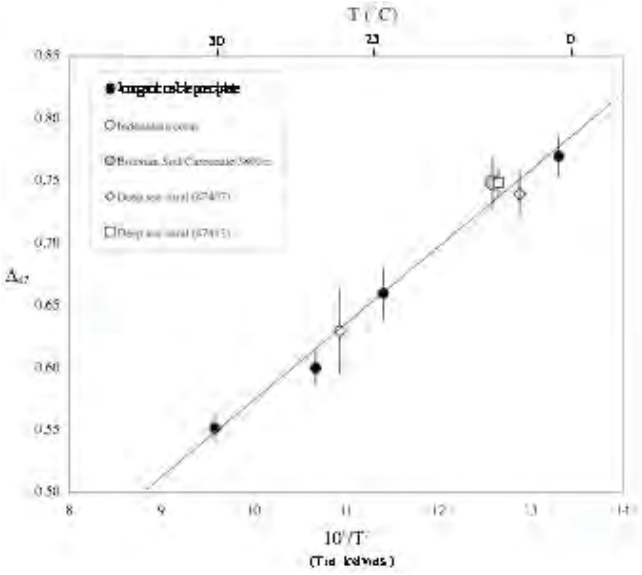

Figure 11. Data documenting the calibration of the carbonate clumped-isotope thermometer for inorganic calcite grown in the laboratory (filled circles) and aragonitic corals grown in nature at known temperatures (an example of one of several biogenic materials we have also calibrated; unfilled symbols). The large, gray circle shows the result of analyses of a modern soil carbonate collected from the Bolivian Altiplano plateau. The horizontal position of this data point is based on the mean annual surface temperature near the site of collection between 2004 and the present.

Advantages and disadvantages

Carbonate clumped-isotope thermometry brings several significant capabilities to the problem of paleoelevation reconstruction. Most importantly, the thermometer is based on the thermodynamics of a homogeneous reaction, involving a reaction among components of a single phase. Therefore, the temperature of carbonate growth is defined rigorously by analysis of the isotopic constituents of carbonate alone, or, more precisely, CO_2 produced from that carbonate. Nothing need be known about the isotopic composition of water from which carbonate grew to determine the temperature of carbonate growth.

Secondly, the material analyzed to determine growth temperature is the same as that used to define the $\delta^{18}O_{sc}$ value (in fact, the two measurements are made simultaneously on the same aliquot of CO_2). Because one knows the growth temperature from Δ_{47} measurements and $\delta^{18}O_{sc}$ values through conventional measurements, one can calculate the $\delta^{18}O_{sw}$ value from which it grew based on the known temperature dependence of the carbonate-water oxygen isotope fractionation (e.g., Kim and O'Neil 1997). Thus, clumped isotope thermometry, combined with conventional stable isotope geochemistry, provides two complementary bases for estimating paleoelevation: comparison of the record of carbonate growth temperatures with inferred altitudinal gradients in surface temperature, and comparison of calculated values of the $\delta^{18}O_{sw}$ with inferred altitudinal gradients in the $\delta^{18}O_{mw}$ values.

Finally, the correlation of calculated $\delta^{18}O_{sw}$ values with carbonate growth temperature imposes one more potentially useful constraint: the slope of this trend, $\partial\delta^{18}O_{water}/\partial T$, for an altitudinal transect is, in many cases, a known or predictable quantity that differs from slopes resulting from variations in season, latitude or climate (Ghosh et al. 2006b; see also Figure 15 of this chapter). Therefore, knowledge of this slope for a suite of related pedogenic carbonates can potentially distinguish between variations in surface temperature and/or the $\delta^{18}O_{mw}$ value caused by changes in elevation versus variations caused by other factors. In practice, this constraint will be more useful in some cases than in others because of natural variations in $\partial\delta^{18}O_{water}/\partial T$ slopes for processes of interest, and because some suites of pedogenic carbonates will be influenced by more than one factor. Nevertheless, it provides another basis for improving the confidence and precision of paleoelevation estimates.

Approaches to paleoelevation reconstruction based on carbonate clumped isotope thermometry also carry with them several disadvantages, most importantly, that the analytical techniques involved in a clumped isotope paleotemperature estimate (Eiler and Schauble 2004; Affek and Eiler 2006; Ghosh et al. 2006b) are slow, technically difficult, and presently made in only one laboratory. It seems likely that these measurements will become more routine as they are adopted in other laboratories and improved through various possible innovations (such as automation). Nevertheless, the supply of data is a limitation at present. Secondly, the precision of data is poor for some problems. This too appears likely to improve through time (e.g., Came et al. in review) report carbonate clumped isotope measurements with precisions corresponding to errors of only ± 0.9 °C), but will remain a significant issue for the foreseeable future due to the subtle temperature sensitivity of isotopic clumping in Reaction (1). Finally, because carbonate clumped isotope thermometry is a relatively new technique, the potential exists that there are unrecognized systematic errors in its application to pedogenic carbonates, such as unexpected fractionations during pedogenic carbonate growth, or poor preservation.

Diagenesis

Any attempt to reconstruct elevation using geochemical proxies must consider the possibility that diagenesis and burial metamorphism have overprinted the carbonate record. The $\delta^{18}O$ values of all carbonates are quite susceptible to diagenetic alteration, as witnessed by the extraordinary difficulty in reconstructing $\delta^{18}O$ values of sea-water through deep geologic time using carbonates, as contrasted with, for example, $\delta^{13}C$ values and $^{87}Sr/^{86}Sr$ ratios (e.g., Veizer et al. 1999). Carbonates buried to depths of several km or less can be overprinted through dissolution and re-precipitation reactions with ground and formation waters. The best approach to evaluating the potential effects of diagenesis depends on the material under study. For example, studies that use non-marine shells can take advantage of the fact that unaltered shell retains its primary structure (Veizer et al. 1999) and has not been converted to calcite from aragonite. In the case of soil nodules, recrystallization to spar is a clear warning sign, since the primary texture of pedogenic carbonate is mostly micritic to microsparitic (Chadwick et al. 1988; Deutz et al. 2002; Garzione et al. 2004). These replacement textures can be identified with the naked eye, optical microscope or cathodoluminiscope, and avoided by sampling

with a slow-speed drill or similar tool, as in both our Andean and Tibet studies discussed below. This strategy appears to be sufficient for recovering records of primary variation in $\delta^{18}O_{sc}$ and $\delta^{13}C_{sc}$ values (e.g., Koch et al. 1995). However, there is no means of knowing, *a priori*, whether this approach will avoid overprinting of the ^{13}C-^{18}O ordering that governs the carbonate clumped isotope thermometer. Hence, in the next section on the Andes we discuss other ways to evaluate the fidelity of the clumped isotope thermometer.

Another approach to diagenesis discussed in the final section of this paper is to look for heterogeneity in $\delta^{18}O_{sc}$ values of adjacent calcitic phases such as interbedded marine, detrital (Quade and Cerling 1995), lacustrine (e.g., Cyr et al. 2005; DeCelles et al. 2007a), and paleosol carbonates. The concept here is that diagenesis should tend to homogenize $\delta^{18}O$ values that in a primary state may have had very different values.

PALEOSOL RECORDS OF PALEOELEVATION CHANGE: CASE STUDIES

We now turn to published and unpublished results of case studies from the Andes and Asia as illustrations of how $\delta^{18}O_{sc}$ and Δ_{47} measurements from paleosol carbonates can be used in paleoelevation reconstruction. The key points that we address include: (1) accounting for the role of climate change in reconstructing paleoelevation; (2) testing for diagenetic alteration of primary $\delta^{18}O_{cc}$ values due to burial in deep sedimentary basins; (3) evaluating paleoaridity, and therefore extent to which evaporation has increased the $\delta^{18}O_{mw}$ values of paleowaters, producing underestimates of paleoelevation, (4) comparing pedogenic carbonate records to other sedimentary carbonates to determine the fidelity of various elevation proxies, and (5) the power of combining conventional $\delta^{18}O_{mw}$ and Δ_{47} measurements in paleoelevation reconstruction.

Paleoelevation reconstruction of the Bolivian Altiplano

We can combine both $\delta^{18}O$ and Δ_{47} measurements of pedogenic carbonate from the Miocene deposits of Bolivia to trace uplift of the Bolivian Altiplano through time. The northern Altiplano is an attractive target for both approaches to paleoelevation reconstruction for several reasons. It preserves carbonate-bearing sediments deposited over much of its uplift history; the modern altitudinal gradients in temperature and the $\delta^{18}O_{mw}$ values are known (Gonfiantini et al. 2001), providing a locally calibrated basis for reconstructing past elevation; modern rainfall rates are > 250 mm/yr, providing adequately wet conditions to reconstruct meteoric water compositions; previous studies of the mountain belt history and geomorphology of the Altiplano provide observations that can be used to test and elaborate on one's results; and, the amplitude of elevation change is large (several km) and thus the analytical precision of clumped isotope measurements is not a severe limitation.

The Altiplano basin is a broad internally drained basin that occupies the central Andean plateau between 15°S and 25°S. At an average elevation of ~3800 m, the Altiplano is situated between the Eastern and Western cordilleras that reach peak elevations in excess of 6 km (Figs. 1a, 2a). The Western Cordillera is the modern magmatic arc of the Andes, and the Eastern Cordillera is a fold-thrust belt made up of deformed Paleozoic metasedimentary rocks. The Altiplano basin has been internally drained since at least late Oligocene time, evidenced by both westward paleoflow and derivation of sedimentary sources from the Eastern Cordillera (Horton et al. 2002; DeCelles and Horton 2003). The late Miocene stratigraphic sections near Callapa are ~3500 m thick and are exposed in the eastern limb of the Corque synclinorium. Three measured sections include fluvial and floodplain deposits in the lower 1200 m and the upper 800 m and widespread lacustrine deposits (laterally continuous for more than 100 km along strike) in the middle part of the section (Garzione et al. 2006). Age constraints on these rocks come from $^{40}Ar/^{39}Ar$ dates on tuffs within our measured section (Marshall et al. 1992) and magnetostratigraphy (Roperch et al. 1999; Garzione et al. 2006).

Fluvial-floodplain and lacustrine sediments contain authigenic carbonates for which $\delta^{18}O_{sc}$ values and $\delta^{13}C_{sc}$ values were obtained (Garzione et al. 2006). The floodplain deposits contain both paleosol carbonate nodules and palustrine carbonates. Paleosols are massive and red to reddish brown. Discrete carbonate (Bk) horizons include rare carbonate rhizoliths and occur below the upper part of the B horizon that has been leached of carbonate. Paleosol carbonate nodules, 0.5 to 3 cm in diameter, were sampled between ~20 and 80 cm below the top of the paleosol where their depth within the soil profile could be measured. In many instances, it was not possible to determine the top of the soil profile because, in general, floodplain lithofacies show extensive oxidation and pedogenesis that makes it difficult to identify the top of individual soil profiles. Palustrine carbonates represent marsh or shallow pond deposits in the floodplain adjacent to fluvial channels. These laminated, mud-rich micrites presumably precipitated seasonally when evaporation rates and productivity were higher. Within the lacustrine interval in the middle part of the section, carbonates are rare and include laminated, very thinly bedded, micritic limestone that contains vertical worm burrows and laminated, thinly to thickly bedded, calcareous mudstone. In thin section, paleosol, palustrine, and lacustrine carbonates lack sparry calcite, suggesting that they have not undergone extensive, late-stage diagenesis. This inference is supported by Δ_{47} paleothermometry data that indicate that pedogenic carbonates do not show a systematic increase in formation temperature with burial depth (Eiler et al. 2006; **Fig. 12**).

Garzione et al. (2006) excluded lacustrine carbonates from their paleoelevation analysis while including palustrine and pedogenic carbonates. Both modern and ancient lake studies show that closed-basin lakes, such as the paleolake that occupied the northern Altiplano in late Miocene time, experienced moderate to extreme evaporative enrichments in the ^{18}O of

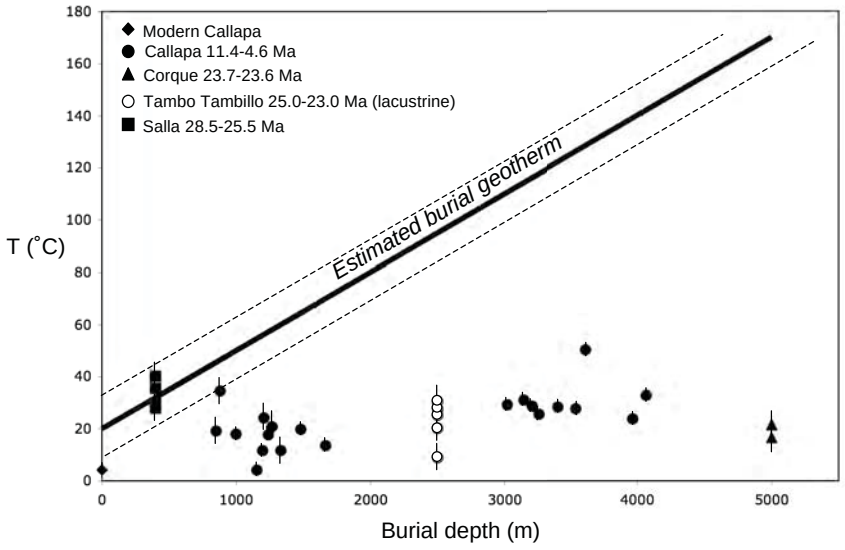

Figure 12. Apparent growth temperatures for various Altiplano carbonates based on clumped isotope thermometry, plotted as a function of estimated maximum burial depth. Symbols discriminate among soil carbonates from sections near Callapa, Corque and Salla and lacustrine carbonates from near Tambo Tambillo, as indicated by the legend. The heavy solid line indicates an estimated burial geotherm, assuming a surface temperature of 20 °C and a gradient of 30 °C per km. The dashed lines define a ±10° offset from this trend, which we consider a reasonable estimate of its uncertainty. Carbonates deposited within the last 28.5 Ma and buried to 5000 meters or less exhibit no systematic relationship between apparent temperature and burial depth, and show no evidence for pervasive resetting of deeply buried samples. Error bars are ±1σ (when not visible, these are approximately the size of the plotted symbol).

water and carbonate that precipitated from it (e.g., Talbot 1990). Studies in the Altiplano region support the inference that closed-lake waters in the Altiplano and Eastern Cordillera have higher values of $\delta^{18}O$ than local rainfall (Wolfe et al. 2001). In addition, Altiplano lacustrine deposits contain abundant gypsum suggestive of extreme evaporation that would systematically bias carbonates toward lower estimates of paleoelevation. Comparing lacustrine deposits to paleosol carbonates above and below the lacustrine interval shows that $\delta^{18}O_{mw}$ values of lacustrine carbonates are on average 2.8‰ to 3.8‰ higher than pedogenic carbonates (**Table 1**), which reinforces the notion that they record the effects of evaporative enrichment in ^{18}O. Palustrine carbonates form in settings comparable to open-basin lakes through which water flows and where evaporative enrichment is much less than in closed basins. These depositional environments are in communication with river waters, lack interbedded gypsum, and therefore should not be as evaporitic. Despite lack of evidence for extreme evaporation, these carbonates generally record $\delta^{18}O$ values that are ~1‰ higher than $\delta^{18}O_{sc}$ values of similar age (Table 1). The consistently lower $\delta^{18}O_{sc}$ values indicate that paleosol carbonates are probably the most faithful recorders of the isotopic composition of meteoric water and therefore provide the best estimates of paleoelevation.

In modern soils globally, $\delta^{13}C_{sc}$ and $\delta^{18}O_{sc}$ values covary, with higher δ values reflecting more arid conditions and lower respiration rates (Cerling 1984; Quade et al. 1989a; Deutz et al 2002). In contrast, within the Altiplano basin, $\delta^{13}C_{sc}$ values increase at 7.6 Ma, whereas $\delta^{18}O_{sc}$ values decrease (**Figs. 13**a and b). A plot of $\delta^{18}O$ values versus $\delta^{13}C$ values (Fig. 13c) (excluding one outlier) show an inverse relationship between $\delta^{18}O$ and $\delta^{13}C$ values ($R^2 = 0.37$). The timing of the increase in $\delta^{13}C$ values could be interpreted to reflect lower soil respiration rates (e.g., Cerling and Quade 1993) or an increasing proportion of C_4 grasses in the Altiplano at this time, coincident with the global expansion of C_4 grasses (Cerling et al. 1997; Latorre et al. 1997). Analysis of both modern and fossil tooth enamel of large grazing mammals in the Altiplano shows no evidence for significant C_4 presence in the region today or at any time in the

Table 1. Oxygen and carbon isotope data from stratigraphic sections sampled in the eastern limb of the Corque syncline (from Garzione et al. 2006).

Sample type	$\delta^{18}O$(VPDB) (mean ‰ ± 1σ)	$\delta^{13}C$(VPDB) (mean ‰ ± 1σ)	# of samples
11.5 to 10.3 Ma			
paleosols	−11.8 ± 0.9	−9.0 ± 1.0	14
palustrine	−10.9 ± 1.5	−8.2 ± 0.8	9
10.1 to 9.1 Ma			
lacustrine	−9.0 ± 1.3	−8.8 ± 3.2	21
7.6 to 6.8 Ma			
paleosol	−12.8 ± 0.9	−4.3 ± 2.1	2
palustrine	−11.3 ± 1.4	−8.4 ± 1.6	12
6.8 to 5.8 Ma			
paleosol	−14.7 ± 0.7	−6.1 ± 1.0	4
s.s. cement	−14.8 ± 0.4	−8.6 ± 1.2	5

Standard deviation (1σ) of the mean of each sample set is reported. VPDB - Vienna Peedee belemnite. Two pedogenic carbonate data points have been excluded, one that shows much higher temperatures relative to other pedogenic nodules of the same age (based on Δ_{47} measurement) and one that has a much higher $\delta^{18}O$ relative to other pedogenic nodules of the same age.

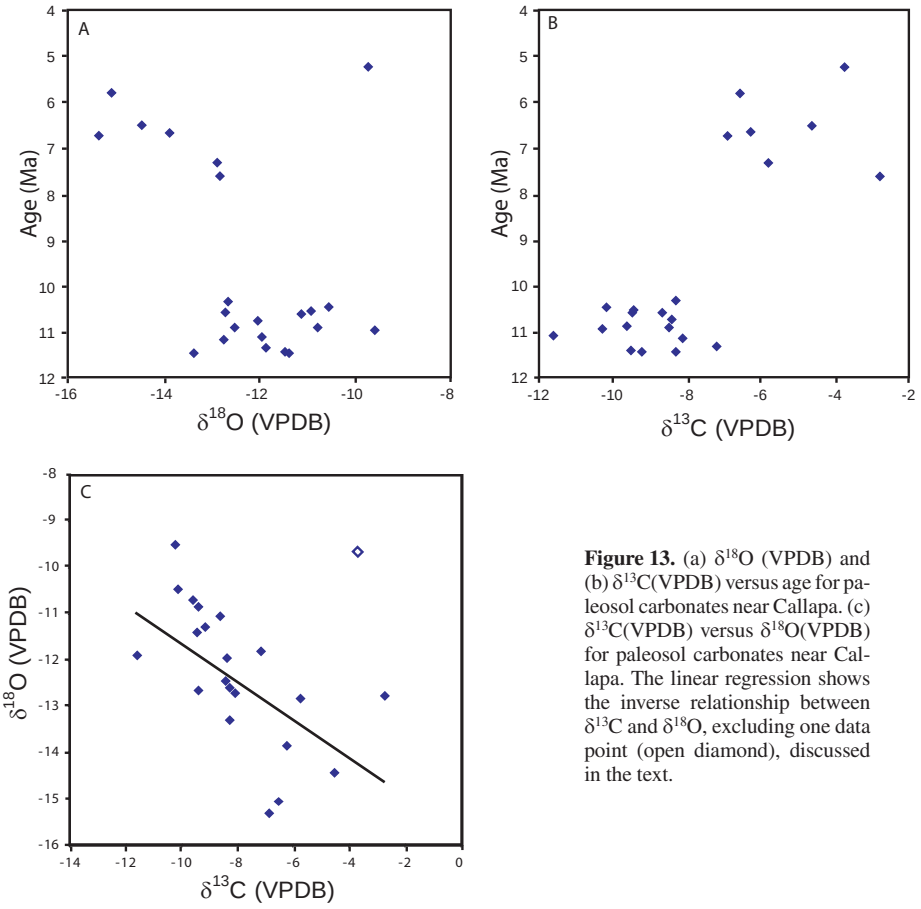

Figure 13. (a) $\delta^{18}O$ (VPDB) and (b) $\delta^{13}C$(VPDB) versus age for paleosol carbonates near Callapa. (c) $\delta^{13}C$(VPDB) versus $\delta^{18}O$(VPDB) for paleosol carbonates near Callapa. The linear regression shows the inverse relationship between $\delta^{13}C$ and $\delta^{18}O$, excluding one data point (open diamond), discussed in the text.

past 8 Myr (Bershaw et al. 2006). Therefore, an increase in the proportion of C_4 grasses is an unlikely cause for the observed increase in $\delta^{13}C_{sc}$ values. We suggest that this increase may be the result of lower respiration rates due to increasingly arid conditions in the Altiplano.

Increasing aridity in Altiplano basin is supported by several lines of evidence from the sedimentary record. First, both the thickness of fluvial channel deposits and their lateral continuity decrease up-section. In the oldest part of the section, channel sandstone bodies up to 15 m thick continue laterally for 100s of meters. Internally, these sand bodies consist of amalgamated lenticular beds that show low-angle cross stratification, interpreted to reflected lateral accretion on migrating longitudinal bars. Individual bar deposits are up to 2 m thick, reflecting the maximum channel depth during high discharge events. Above the lacustrine interval, channel sandstone bodies are up to 5 m thick and continue laterally for tens of meters. Individual beds often contain trough cross-stratification and are <1 m thick, indicating shallower channel depths compared to older deposits. Both shallower channel depths and a decrease in the lateral extent and overall thickness of sandstone channel deposits suggest lower discharge in the fluvial systems above the lacustrine interval. The second line of evidence comes from the depth of pedogenic carbonate formation. Below the lacustrine interval, pedogenic carbonates were observed to have formed below 30 cm in the paleosol profile, whereas pedogenic

carbonates formed at depths as shallow as 16 cm in paleosols above the lacustrine interval. The observation in Holocene soils that depth to the Bk horizon increases with increasing mean annual precipitation (Royer 1999) suggests that the youngest part of the soil record reflects the most arid conditions. The combined observations of increased aridity in late Miocene time point to lower soil respiration rates as the cause of the increase in $\delta^{13}C$ values up section.

We revise and update paleoelevation estimates for the northern Altiplano here and in the following section on "clumped isotope thermometry." Realizing that Gonfiantini et al. (2001) mislabeled data in their Table 5 as weighted means, when they are in fact unweighted means, we estimate elevation as in Garzione et al. (2006) using the weighted mean values for 3 years of rainfall data reported in Table 6 of Gonfiantini et al. (2001). Seven sites for which rainfall amount was also reported can be used for the regression. The linear regression to these data is:

$$h = -472.5\delta^{18}O_{mw} - 2645 \quad (4)$$

where h = elevation in meters, and with an $r^2 = 0.95$ (Fig. 2a, 14). We choose a linear regression because there are not enough data points in the weighted mean data set to evaluate whether a polynomial provides a better fit to the data. Surface water data collected over 2004 and 2005 years from small tributaries along the Coroico River, where rainfall samples were collected, agree with the weighted mean values observed in the sparse rainfall data set and show a similar isotopic gradient to Equation (4), which indicates that the isotopic gradient observed in meteoric water is reflected in surface water. Use of Equation (4) produces elevation estimates of: 400 to 2200 m in carbonates deposited before 10.3 Ma, 2000 to 3800 m in carbonates deposited between 7.4 Ma and 6.8 Ma, and 4000-4700 m in carbonates deposited after 6.8 Ma. This reanalysis of the data based on weighted mean precipitation suggests essentially the same amount of surface uplift (2.5 to 3.6 km) as our original estimates of 2.5 to 3.5 km. It also brings the calculated elevations for the oldest part of the section into a more reasonable range,

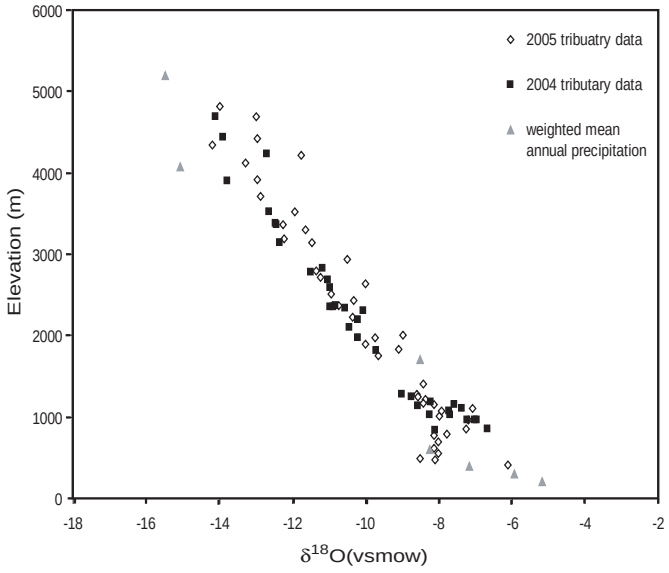

Figure 14. $\delta^{18}O$ (VSMOW) of rainfall and surface waters across the Eastern Cordillera. Rainfall data represent the weighted mean isotopic composition (1983-1985) from Gonfiantini et al (2001). Tributaries to the Coroico river were sampled in late May 2004 and early May 2005 and are plotted relative to the sampling elevation. A linear regression to the rainfall data (gray triangles) defines Equation (4) in the text.

with all values above 400 m, as opposed to the negative elevations calculated for the oldest part of the record in Garzione et al. (2006). Given that paleoelevation estimates are prone to systematic biases that tend to underestimate elevations, we suggest using the difference between the highest elevation estimates prior to 10.3 Ma and after 6.8 Ma of 2.5 km as a conservative estimate for the amount of late Miocene surface uplift, with an uncertainty of ±1 km (see Rowley and Garzione 2007 for discussion of uncertainties)

Ideally, to apply stable isotopes to paleoelevation reconstruction, low-elevation records of regional climate are required to constrain variations in climate that may influence the isotopic record. For example, the Siwalik foreland basin deposits south of the Himalaya provide low-elevation constraints on climate and the isotopic composition of meteoric water used to estimate elevations in southern Tibet (Garzione et al. 2000a; Rowley at al. 2001; Currie et al. 2005). The accuracy of the current estimates of paleoelevation of the Altiplano is limited by lack of data from simultaneous low elevation records in the Subandean foreland (Rowley and Garzione 2007). Several potentially confounding variables that are currently unconstrained are the proximity and isotopic composition of sources of water vapor, secular changes in terrestrial temperature associated with late Cenozoic cooling, and the effects of climate change on the isotopic lapse rate. Because of extensive evapotranspiration over the Amazon basin, modern water vapor delivered to the eastern flank of the Andes is isotopically similar to water vapor at the Atlantic coast (Vuille et al. 2003). However, the continental isotopic gradient may have changed through time as a result of changes in plant cover and/or changes in the extent and nature of inland water bodies in the Amazon basin. Recent studies document a late Miocene marine incursion in the northern Subandean foreland. Although these marine rocks lack precise age constraints, Hernández et al. (2005) show that at least one marine unit was slightly younger than 7.7±0.3 Ma. Hernández et al. (2005), Uba et al. (2006), and Hoorn (2006) show that marine conditions existed briefly, while lacustrine conditions prevailed for longer time periods. A lacustrine origin is supported by stable isotopic evidence that indicates a predominantly Andean freshwater and cratonic freshwater origin for the water isotopic composition recorded in microfossils deposited between 18°S and 19°S (Hulka 2005). The changing paleogeography of the Andean foreland points to the need to better establish foreland records of both climate and paleogeography to more accurately constrain paleoelevation of the Altiplano in late Miocene time.

Results from clumped isotope thermometry

Burial effects. Eiler et al. (2006) examined the effects of post-depositional alteration on the carbonate clumped isotope thermometer in soil and lacustrine carbonates from the northern Altiplano, spanning a range in age from 0 to 28.5 Ma and maximum burial depths from ~0 to ~5 km. Age and burial depth estimates for these samples are based on data presented in MacFadden et al. (1985), Kennan et al. (1995), Kay et al. (1998), Garzione et al. (2006), and Ghosh et al. (2006b) and on unpublished magnetostratigraphic, U-Pb geochronologic, and stratigraphic data summarized in Eiler et al. (2006). The results (Fig. 12) demonstrate that the temperatures recorded by carbonate clumped isotope thermometry are uncorrelated with burial depth, generally (i.e., with one exception) indistinguishable from earth-surface temperatures, and preserve temperatures as low as ca. 20 °C in pedogenic carbonates as old as 23.6-23.7 Ma and buried as deep as 5 km. No systematic differences in apparent temperature were observed between soil and lacustrine carbonates, suggesting that the thermometer is insensitive to variations in textural characteristics such as grain size and porosity that might influence susceptibility to overprinting. These results suggest that burial diagenesis has no systematic effect on the temperatures recorded by the carbonate clumped isotope thermometer in micritic portions of pedogenic carbonates over timescales of tens of millions of years and up to burial temperatures approaching 200 °C. Nevertheless, there are reasons to remain cautious when applying this approach to new suites, because one of the samples originally examined by

Ghosh et al. (2006b) recorded a temperature of 50 °C—higher than any plausible depositional temperature. This result is not representative of the record as a whole, but clearly indicates the possibility for overprinting during burial. Moreover, the samples in Figure 12 collected near Salla are shallowly buried but record temperatures that could lie on a burial geotherm. Eiler et al. (2006) speculate that hydrothermal activity associated with nearby ~15-25 Ma magmatism might have partially or completely overprinted these samples.

Paleoelevations of pedogenic carbonate from the Corque syncline

Only the 11.4 to 4.6 Ma paleosols exposed in the Callapa section (Figs. 1a, 12) of the Corque syncline have been studied in enough detail to justify a detailed reconstruction of elevation history. Ghosh et al. (2006b) present such a reconstruction, which we now review. Our discussion of these data differs in some respects from that presented in Ghosh et al. (2006b) because we have re-evaluated the constraints on long-term climate change (which influences the low-elevation "base line" of a paleoalitutude estimate) and re-calculated the elevation trend to $\delta^{18}O_{mw}$ values across the central Andes today. Figure 12 includes data for Callapa pedogenic carbonates from two sources; those from Ghosh et al. (2006b) were analyzed with a relatively high degree of replication and have uncertainties in Δ_{47} equivalent to ±2 to 3 °C, whereas data from Eiler et al. (2006) were not as thoroughly replicated and have uncertainties in apparent temperature averaging ±5 °C. This latter data set is sufficiently precise to test for burial metamorphic overprinting (Fig. 12), but provides inferior constraints on paleoelevation. We therefore focus our discussion on the data from Ghosh et al. (2006b).

Ghosh et al. (2006b) found that pedogenic carbonates from Corque syncline paleosols deposited between 11.4 and 10.3 Ma record carbonate precipitation temperatures of 28.4 ± 2.6 °C (standard error, or s.e., of ±0.9 °C); those grown between 7.6 and 7.3 Ma record temperatures of 17.7 ± 3.1 °C (s.e. of ±2.2 °C); and those grown between 6.7 and 5.8 Ma record temperatures of 12.6 ± 5.6 °C (s.e. of ±2.8 °C). This range in apparent temperature through time is broadly similar to the modern temperature variation with elevation between the east flanks of the Andes and the Altiplano, suggesting that the Altiplano may have risen from low elevation (ca. 1 km or less) to its modern elevation (ca. 4 km) between 10.3 and 6.7 Ma. Note that apparent temperatures for pedogenic carbonates grown between 11.4 and 10.3 Ma are at the high end of modern temperature variations at low elevations on the flanks of the Andes. This could reflect a warmer Miocene climate and/or preferential growth of paleosol carbonates during the austral summer. If we neglect this complicating factor, these data suggest cooling of 15.7 ± 2.9 °C (±1 se). Given the modern gradient in temperature with elevation in the Andes today (4.66 °C/km; Gonfiantini et al. 2001 and data compiled at www.climate-zone.com), this change is consistent with uplift of 3.4 ± 0.6 m, for an average uplift rate of 0.94 ± 0.17 mm/yr between 10.3 and 6.7 Ma. Differences in climate and latitude can account for anywhere between 1.3 °C (Savin et al. 1975; Smith et al. 1981, Zachos et al. 2001) and 2.3 °C (Berner and Kothavala 2001) of the observed temperature change. If we correct for this systematic error, then the amount of cooling due to elevation change could be a minimum of 13.4 ± 2.9 °C (assuming a 2.3 °C change in low-elevation mean annual temperature, all between 10.3 and 6.7 Ma), implying elevation gain of 2.9 ± 0.6 m and an uplift rate of 0.80 ± 0.17 mm/yr.

The contrast in $\delta^{18}O$ (SMOW) values of waters in equilibrium with 11.4 to 10.3 Ma pedogenic carbonates (average −8.6 ± 0.4‰, ± 1 s.e.) versus those in equilibrium with 6.7 and 5.8 Ma pedogenic carbonates (average −14.6 ± 0.6‰, ± 1 s.e.) is 6.0 ± 0.7‰, (± 1 s.e. in the difference of the means). The modern gradient in the annual weighted average $\delta^{18}O_{mw}$ values on the slopes of the Andes (equation 4) implies an elevation gain of 2.8 ± 0.3 km (from 1.4 ± 0.2 to 4.2 ± 0.3 km) between 10.3 and 6.7 Ma, or an uplift rate of 0.78 ± 0.08 mm/yr.

Figure 15 plots the growth temperatures of Corque syncline pedogenic carbonates versus the $\delta^{18}O$ values of waters from which they grew, and compares the trend in those data to the modern trends in surface temperatures and meteoric water $\delta^{18}O$ values across a range of elevations in the

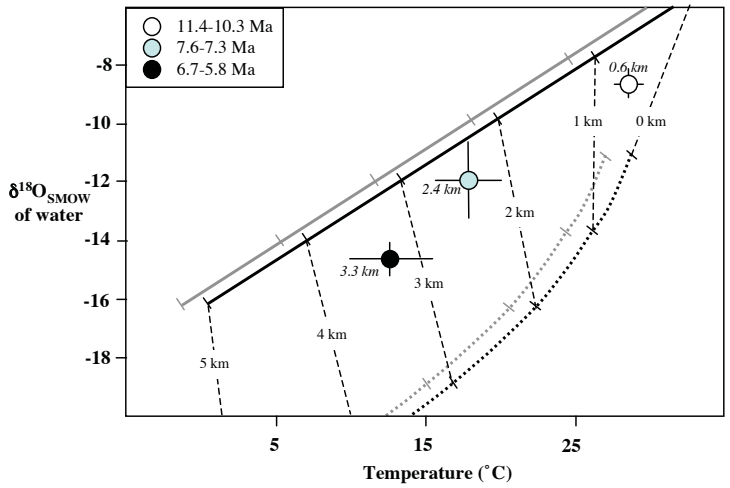

Figure 15. Plot of the $\delta^{18}O_{SMOW}$ value of water in equilibrium with soil carbonate nodules vs. the growth temperatures of those nodules. Circles are averages for the 11.4-10.3 Ma, 7.6-7.3 Ma and 6.7-5.8 Ma age groups, as indicated in the legend. Error bars are ±1 standard error of the population. Gray lines show the mean annual trend (solid) and trend of Jan/Feb extreme (dotted) for the modern relationships between surface temperature and $\delta^{18}O_{SMOW}$ of meteoric water. These trends are contoured for altitude in 1-km increments. The similar heavy and dotted black trends plot the expected location of the mean annual and Jan/Feb extremes in the mid-Miocene, based on inferred changes in the latitude of Bolivia, low-latitude climate change and secular variation in the $\delta^{18}O$ of sea water (Savin et al. 1975; Smith et al. 1981). Fine dashed lines connecting the mid-Miocene mean annual trend and Jan/Feb extreme trend show the slopes of seasonal variations in T and $\delta^{18}O$ of water at a fixed altitude. Paleoaltitudes of age-group averages are estimated by their intersections with this set of altitude contours, as indicated by the italicized text.

central Andes. These modern trends are shown both for the annual weighted mean (solid grey line) and Jan/Feb seasonal extreme (dotted gray line), and have been corrected for differences between the Miocene and today in climate, latitude of the Altiplano and the $\delta^{18}O$ value of the ocean (see the caption to Figure 15 for details). Fine, dashed black contour lines of constant elevation link the mean annual trend with the Jan/Feb extreme for the inferred Miocene trends. This figure is useful in two respects: (1) the fact that the trend defined by data for Miocene pedogenic carbonates parallels the trend for an elevation transect re-enforces the interpretation that variations in pedogenic carbonate growth temperature in the northern Altiplano and $\delta^{18}O$ primarily reflect elevation change rather than other factors (e.g., climate change; latitude change; changing seasonality of pedogenic carbonate growth); and (2) we can use a sample's position in relation to the iso-elevation contours in Figure 15 to estimate its paleoelevation, thereby circumventing systematic errors that could occur if pedogenic carbonates had any variations in the season of growth. This is important because the plot of points in Figure 15 suggests that the season of formation for the pedogenic carbonates examined in this study are biased toward warm, low-$\delta^{18}O$ conditions that prevail in the Bolivian austral summer. Our results suggest that the Altiplano rose 2.7 ± 0.4 km (from 0.6 ± 0.2 km to 3.3 ±0.4 km) between 10.3 Ma and 6.7, implying an average uplift rate of 0.73 ± 0.12 mm/yr.

Paleoatimetry of southern Tibet and the Himalaya

Burial effects. We have been involved in several studies in the Himalaya and Tibet that illustrate the need to carefully evaluate the potential effects of burial metamorphism on $\delta^{18}O_{sc}$ values before using them to reconstruct paleoelevation. The first comes from Penbo in southern Tibet (Fig. 1b) where Leier (2005) analyzed paleosol carbonates in close stratigraphic proximity

(< 200 m) to marine carbonates from the late Cretaceous Takena Formation. This association shows that the Takena paleosols formed near sea-level. The nodules from the paleosols are a mix of micrite with local sparry zones, both of which we analyzed. Both textures yielded $\delta^{18}O_{sc}$ values −12 to −14‰ (Fig. 16). These are implausibly low for a low-latitude coastal site and reflect isotopic exchange, possibly at elevated temperatures, with meteoric waters with very low $\delta^{18}O_{mw}$ values, such as those that occur in the region today. To test this, Leier (2005) analyzed stratigraphically adjacent marine limestone, including spars, micrite, and fossils fragments. Again all phases—from matrix micrite to recrystallized fossils—yielded much lower $\delta^{18}O$ values (−12 to −14‰; Leier 2005; Fig. 16) than expected (0 to −4‰) for late Cretaceous marine carbonates (Veizer et al. 1999). This example clearly illustrates the effects of isotopic homogenization due to burial metamorphism of originally heterogeneous calcite phases.

The second example is unpublished data from paleosol carbonates of the Oligocene-age Dumri Formation in central Nepal (Fig. 1b). The Dumri Formation underlies the better known Siwalik Group, and represents the early stages (Oligo-Miocene) of Himalayan foreland deposition. Non-paleosol carbonates are unavailable from our study sections to check for isotopic homogenization expected from diagenesis. Petrographic evidence shows local but not pervasive recrystallization of paleosol nodules. Most $\delta^{18}O_{sc}$ values, however, are < −17‰, implausibly low given that the paleosols must have formed near sea-level along the ancestral Ganges River and the foreland reaches of its paleo-tributaries. The Dumri Formation at this location experienced deep (> 8 km) tectonic burial under a thick thrust wedge of Greater Himalayan nappe rocks (DeCelles et al. 1998), so resetting of $\delta^{18}O_{sc}$ values at elevated temperatures is unsurprising.

A final example comes from the Nima basin located ~450 km northwest of Lhasa at about 4500 m, in the southern part of the Bangong suture zone, which separates the Qiangtang and Lhasa terranes in central Tibet (Fig. 1b). The southern Nima basin contains more than 4 km of Tertiary alluvial, fluvial, lacustrine, and lacustrine fan-delta deposits that accumulated next to growing thrust-faulted ranges (DeCelles et al. 2007b). Lacustrine marl beds and well-developed calcareous paleosols are common in the informally designated Nima Redbed unit

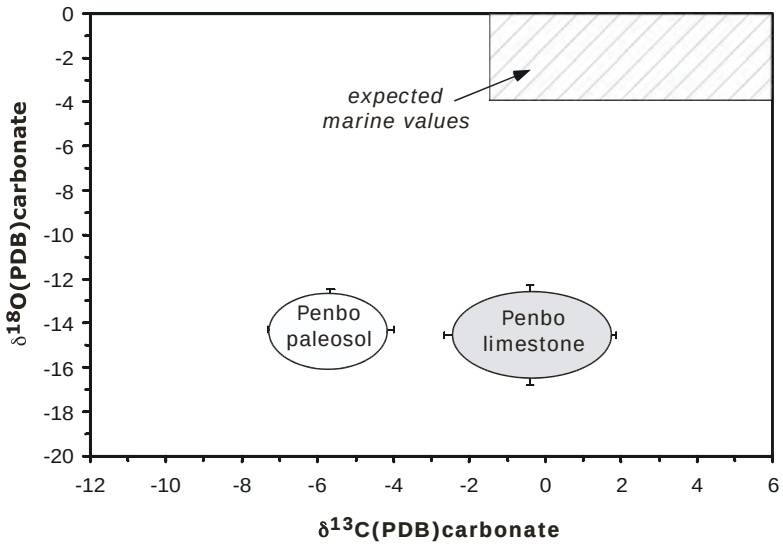

Figure 16. $\delta^{18}O_{sc}$ (PDB) versus $\delta^{13}C_{sc}$ (PDB) values from marine limestone and paleosol carbonate in the late Cretaceous Takena Formation at the Penbo locality, southern Tibet (Leier 2005). Range of expected marine isotopic values for the late Cretaceous from Veizer et al. (1999).

which is exposed in a roughly 50 km-long outcrop belt. For age control, $^{40}Ar/^{39}Ar$ dates from six reworked tuffs in the Nima Redbed unit securely place the age of the analyzed deposits between 25 and 26 Ma (late Oligocene) (DeCelles et al. 2007b).

We devised an "isotopic conglomerate test" in order to assess the potential for diagenetic resetting of the isotopic paleoelevation signal (DeCelles et al. 2007a). The Nima Redbeds contain numerous conglomerates interbedded with the marls and paleosols that we sampled for paleoelevation reconstruction. Among other rock types, these conglomerates contain abundant marine limestone clasts derived from the Lower Cretaceous Langshan Formation cropping out around the basin. Where paleochannels carrying these gravels scour into contemporaneous marls and paleosols, reworked paleosol carbonate nodules are also present in channel lags. The limestone clasts are composed of both micrite and sparite and commonly contain obviously recrystallized marine fossils. In contrast, the Tertiary lacustrine marls and nodular paleosol carbonates are dense, well-indurated micrite containing well-preserved gastropod, ostracod, and *Chara* fossils.

Our hypothesis is that if resetting by diagenesis has occurred in the Nima basin, carbonates of all types should exhibit uniformly very low $\delta^{18}O_{sc}$ values (< −6‰), owing to diagenetic interaction at higher temperatures with ^{18}O-depleted meteoric water that is characteristic of recharge in the region today. Critical here is that clasts of marine limestone should not retain their primary marine $\delta^{18}O_{sc}$ values of > −5‰ (Veizer et al. 1999), as observed in the example from the upper Cretaceous Takena Formation.

Analysis of the reworked Cretaceous marine limestone pebbles and cobbles yielded several $\delta^{18}O_{sc}$ values > −3‰ (**Fig. 17**), in the range expected for unaltered Cretaceous marine carbonates. This indicates that some of the limestone pebbles are not diagenetically reset despite a long history of uplift, erosion, and burial over a time period of approximately 80 million years. Other Cretaceous-age limestone pebbles yielded $\delta^{18}O_{sc}$ values ranging between −5‰ and −15‰, indicating that they have been diagenetically reset by interaction with meteoric waters (Fig. 17). In sharp contrast, paleosol carbonate nodules—both reworked and *in situ*—in the Nima basin yielded tightly clustered $\delta^{13}C_{sc}$ values of −3.5 ± 0.6‰ (range −2.3 to −4.6‰; n = 31) and $\delta^{18}O_{sc}$ values of −17.0 ± 0.3‰ (range −16.3 to −17.5‰). The large spread in $\delta^{18}O$ values of the marine limestone clasts, as contrasted with the narrow range of values from *in situ* and reworked Nima paleosol carbonate (Fig. 17), indicates that resetting of the limestone must have occurred prior to deposition in the Nima basin, during previous burial of the limestone. Thus, we interpret paleosol carbonate in the Nima basin as preserving the original isotopic composition of meteoric water during the late Oligocene.

Results from marl and fossil Chara and ostracodes in section with the paleosols strongly reinforce the view that the paleosol carbonates are preserving primary values. Marls range in $\delta^{18}O$ values between −16.5 to −8.9‰, whereas those from fossil *Chara* and ostracodes fall between −18.1 to −4.7‰. The most negative values are very similar to those from pedogenic carbonates. The large spread in $\delta^{18}O$ values is consistent with periodic strong evaporation in the Nima paleolake. The most positive $\delta^{18}O$ values from fossils and marl are very similar to carbonate forming in modern Tibetan lakes (Quade, unpublished data).

Paleoaridity. As already discussed, we can use $\delta^{13}C_{sc}$ values from paleosols as potential archives of paleoaridity. Unlike $\delta^{18}O_{sc}$ values, $\delta^{13}C_{sc}$ values in carbonates are far less prone to diagenetic resetting because of the very low carbon (versus high oxygen) content of natural waters. Results from the upper Cretaceous Takena Formation cannot be used to reconstruct paleoaridity, because of much higher pCO_2 at that time (Ekart et al. 1999). However, results from the late Oligocene to early Miocene Dumri Formation and Nima redbeds are admissible.

$\delta^{13}C_{sc}$ values from the Dumri Formation average −10.3 ± 0.6‰. These very low values are similar to those obtained from the overlying Siwalik Formation in paleosols > 8 Ma. They

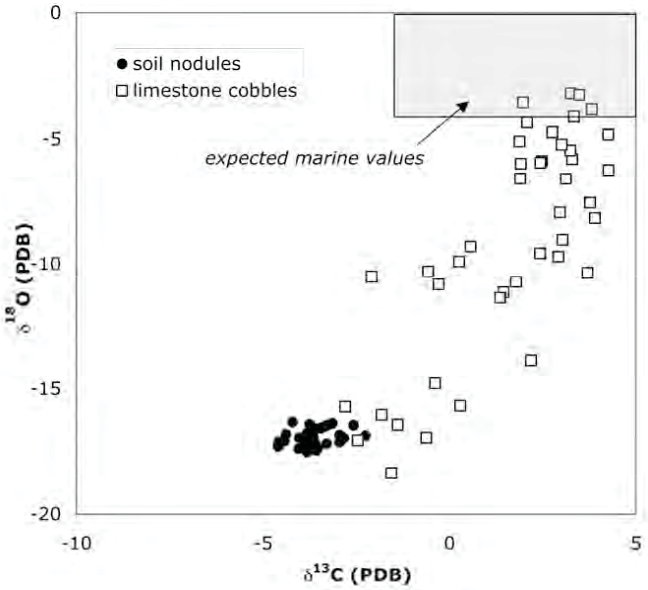

Figure 17. $\delta^{18}O_{sc}$ (PDB) versus $\delta^{13}C_{sc}$ (PDB) values from marine limestone cobbles (variable ages) and paleosol carbonate in the late Oligocene-age Nima Redbeds, southern Tibet (DeCelles et al. 2007a). Range of expected marine isotopic values for the late Cretaceous from Veizer et al. (1999).

imply high respiration rates of 4-8 mmoles/m^2/hr, assuming $\delta^{13}C$ values of local plants between −24 and −25‰. This in turn indicates moist climatic conditions, consistent with paleobotanic evidence for the period (Lakhanpal 1970).

By contrast, $\delta^{13}C_{sc}$ values from Nima paleosols in central Tibet (Fig. 1b) formed at about the same time as those in the Dumri Formation, but on the other side of the Himalaya, and are much higher (−3.5 ± 0.6‰). These results are very close to the lowest $\delta^{13}C_{sc}$ values from modern pedogenic carbonates from immediately around Nima, which range from −3.4 to +7.7‰. The relatively high $\delta^{13}C_{sc}$ values for modern carbonates indicate mixing of atmospheric CO_2 with plant-derived CO_2 owing to low soil respiration rates, a result of arid local climate of ~200-250 mm/yr. Similarly, the high $\delta^{13}C_{sc}$ values from paleosol carbonates indicate very low soil respiration rates at 25-26 Ma (Fig. 6). Ancient soil respiration rates of 0.15 to 0.7 mmoles/m^2/hr can be calculated from the one-dimensional soil diffusion model of Cerling (1984) and modified in (Quade et al. 2007), assuming model conditions given in the caption to Figure 6. These respiration rates are very low and typical of sparsely vegetated, low-elevation settings in the Mojave (Quade et al. 1989a). Aridity in modern Tibet is produced by orographic blockage of moisture arriving from outside the plateau, as well as by orographically induced stationary waves that tend to fix dry, descending air over the plateau during most of the year (Broccoli and Manabe 1992). The high $\delta^{13}C_{cc}$ values from Nima basin paleosols indicate that orographic barriers to moisture also existed during the late Oligocene, most likely the Himalaya, which was actively growing during Oligocene time and earlier.

Paleoelevation. The $\delta^{18}O_{sc}$ values of modern pedogenic carbonate from around Nima (12 analyses, 3 profiles) ranges from −13.8‰ to −6.1‰. $\delta^{18}O_{mw}$ values of meteoric water samples from springs and small creeks in the Nima area at modern elevations of 4500-5000 m range from −12.6‰ to −16.2‰. Using local mean annual temperature of 3°C, $\delta^{18}O$ values of pedogenic carbonate forming in isotopic equilibrium with these waters should be −11.7 to −13.3‰. Thus,

observed (−13.8 to −6.1‰) and predicted (−11.7 to −13.3‰) $\delta^{18}O_{sc}$ values overlap, but modern carbonates exhibit much more positive values (Fig. 10). These high values are consistent with the arid setting of Nima basin (annual rainfall is ~200 mm/yr).

The $\delta^{18}O_{sc}$ values of −17.0 ± 0.3‰ from paleosol nodules are much lower than $\delta^{18}O_{sc}$ values of modern pedogenic carbonate from around Nima of −13.8‰ to −6.1‰ (Fig. 10). On the face of it this would appear to imply higher paleoelevations in the past compared to the present elevation of Nima at ~4500 m. However, this simple comparison is unrealistic because we know that corrections for decreased ice volume, a warmer Earth, lower latitude at 26 Ma, and likely changes in Asian monsoon intensity must be considered. Each of these factors can be considered separately. Or, as in the case of several previous studies (Garzione et al. 2000a; Rowley et al. 2001; Mulch et al. 2004; Currie et al. 2006; Rowley and Currie 2006), changes in $\delta^{18}O_{sc}$ values from a nearby low-elevation site can be used to make the correction. The second approach has great advantages, since it both "anchors" the temperature-$\delta^{18}O_{sc}$ relationship of the paleoclimate system delivering the moisture to Tibet at some known elevation, in this case near sea level, and it subsumes the effects on $\delta^{18}O_{sc}$ values of changes latitude, temperature, global ice volume, and regional climate through time. Critical here is that—today at least— northern India and southern Tibet share a common climate dominated by the SW Indian monsoon.

As with previous studies (Garzione et al. 2000a; Rowley et al. 2001), we can use the data from the Siwalik Group (Quade and Cerling 1995) in the Himalayan foreland of Nepal and Pakistan as our low-elevation reference site. These data only extend back to 17 Ma, since our attempts to extend the lowland isotopic record to the Oligocene failed, as already described. These records show increases in $\delta^{18}O_{sc}$ values in the late Miocene of about 2.5‰, comparing the most negative values (not the means) of the pre-late Miocene pedogenic carbonates (Quade and Cerling 1995). We have interpreted this late Miocene increase in $\delta^{18}O_{sc}$ values as related to a weakening of the Asian monsoon (Dettman et al 2001), the opposite of earlier-held views (Quade et al. 1989b; Kroon et al. 1991; Ruddiman et al. 1997). Causes aside, this ~2.5‰ "correction" can be added to $\delta^{18}O_{sc}$ values from paleosol carbonate (−17‰) at Nima to yield about −14.5‰. This value is slightly lower than the lowest (least evaporated) modern pedogenic carbonate value from Nima of around −13.8‰. On this basis we conclude that $\delta^{18}O_{sc}$ values of paleosol carbonate—after correction—look very similar to modern values. This would imply little change in elevation of the site since the late Oligocene.

Central to our reconstruction is that the $\delta^{18}O_{sc}$ record from Pakistan back to 17 Ma can be applied to late Oligocene Nima, and the shift in the y-intercept of the system (Fig. 2b) of ~2.5‰ encapsulates the changes in global temperature, latitude, sea-water $\delta^{18}O$ values, and monsoon strength over the past 26 Ma. An additional (and related) assumption is that the slope of the modern $\delta^{18}O_{sc}$ value-elevation relationship for southern Tibet has not appreciably changed back through time.

The last assumption is an important one, because just viewing climatic patterns in Tibet today, the slope of the $\delta^{18}O_{sc}$ value-elevation relationship in Tibet is highly dependent on latitude, and should vary according to the strength of the Asian monsoon. For example, a weaker monsoon at 26 Ma should reduce the slope of the $\delta^{18}O_{sc}$ value-elevation relationship in southern Tibet—that is, northerly or local air masses would have had a stronger influence further south in the late Oligocene. This would have the effect of increasing our estimates of paleoelevation compared to today. Alternatively, we might argue that the Asian monsoon was stronger at 26 Ma, resulting in a locally steeper isotopic lapse rates with elevation and overestimated paleoelevation. However, this reasoning is contradictory by invoking a stronger Asian monsoon at 26 Ma in the presence of a lower plateau.

This brings us to our current "best guess" about the Nima record, that paleoelevation in the Oligocene at Nima was at least as high as today, and no higher than today only if the modern Asian monsoon—or something that coincidentally looks a lot like it in oxygen isotope terms

—was already in place at 26 Ma. We would stress, however, that Nima is only one of a handfull of well-dated Oligo-Miocene sites in Tibet (others examples are discussed in Garzione et al. 2000b, Currie et al. 2005, and Rowley and Currie 2006), distributed over a very broad and geologically diverse region. The challenge ahead is to see if our results from Nima and other sites in southern Tibet can be replicated, and to eventually reconstruct the uplift history of the rest of the plateau.

CONCLUDING REMARKS

Paleoelevation reconstruction is a relatively new science. Of the several approaches under development, the use of oxygen isotopes in pedogenic carbonates enjoy several advantages. As to soils themselves, pedogenic carbonate is relatively common in basin deposits of many orogens, especially on the drier leeside. For another, soils form in the presence of local rainfall, and hence are not influenced by the $\delta^{18}O$ value of run-off from higher elevations in the way that, for example, riverine and lacustrine carbonates could be.

The $\delta^{18}O$ analysis of pedogenic carbonate has the advantage of being routine but the major disadvantage of being a function of both temperature and of the $\delta^{18}O$ value of rainfall variably modified by evaporation. Paleoelevation can also be seriously underestimated due to the effects of evaporation. This effect can only be minimized by sampling deep in paleosol profiles and is probably an insurmountable problem in very dry settings (< 200 mm/yr) like the Atacama and low-elevation Mojave Desert. For this reason, Δ_{47} analyses hold much promise because they are only temperature dependent. Here, a final important advantage of soils comes into play: soil *T* collapses to slightly above (+1 to +3 °C) mean annual *T* at soil depth. Other common settings for carbonate formation such as oceans, lakes, and rivers can experience very large temperature swings diurnally or seasonally, and do not converge on mean annual temperature with depth. The combination of $\delta^{18}O$ and Δ_{47} analysis is especially powerful since it provides two largely independent estimates of paleoelevation. Δ_{47} measurements of pedogenic carbonate allow mean annual temperature to be reconstructed, and paleoelevations to be estimated using temperature lapse rates. These same paleotemperature estimates allow $\delta^{18}O_{mw}$ values to be calculated from $\delta^{18}O_{cc}$ values, providing a second estimate of paleoelevation, assuming a local isotopic lapse rate.

Diagenetic resetting poses a serious problem for future paleoelevation reconstructions using carbonate, especially as we delve into the older and deeper geologic record where resetting of $\delta^{18}O$ values is well documented in many situations. Our Tibetan and Bolivian studies offer two approaches to the problem, the Bolivian case where $\delta^{18}O$ and Δ_{47} values provide independent checks of each other, and the Tibetan case by analysis of co-occurring marine limestones.

In the longer view, the $\delta^{18}O$ and Δ_{47} combination entails the fewest assumptions and holds the greatest promise for paleoelevation reconstruction. However, this potential will only be fully realized when Δ_{47} analysis becomes more routine and can be calibrated and tested in very young pedogenic carbonates formed in soils with well-constrained temperature histories.

ACKNOWLEDGMENTS

JQ thanks Paul Kapp and Pete DeCelles for involving him in their Tibetan research, and discussions and data from Dave Dettman and Andrew Leier, and acknowledges support from NSF-EAR-Tectonics 0438115. CG thanks David Rowley and Terry Jordan for insightful discussions, and acknowledges support from NSF-EAR-Tectonics 0230232.

REFERENCES

Affek HP, Eiler JM (2006) Abundance of mass-47 CO_2 in urban air, car exhaust and human breath. Geochim Cosmochim Acta 70:1-12

Allison GB, Barnes CJ, Hughes MW (1983) The distribution of deuterium and ^{18}O in dry soils 2. Experimental. J Hydrol 64:377-397

Allison CE, Francey RJ, Meijer HAJ (1995) Recommendations for the reporting of stable isotope measurements of carbon and oxygen in CO_2 gas. *In:* IAEA-TECDOC-825, Reference and intercomparison materials for stable isotopes of light elements. IAEA, Vienna. p 155-162

Ambach W, Dansgaard W, Eisner H, Mollner J (1968) The altitude effect on the isotopic composition of precipitation and glacier ice in the Alps. Tellus 20:595-600

Amundson R, Chadwick O, Kendall C, Wang Y, DeNiro M (1996) Isotopic evidence for shifts in atmospheric circulation patterns during the late Quaternary in mid-North America. Geology 24:23-26

Araguás-Araguás L, Froelich K, Rozanski K (1998) Stable isotope composition of precipitation over southeast Asia. J Geophys Res 103:28,721-28,742

Aravena R, Suzuki O, Pollastri A (1989) Coastal fog and its relation to groundwater in IV region of northern Chile. Chem Geol (Isotope Geos Sec) 79: 83-91

Aravena R, Suzuki O, Pena H, Pollastri A, Fuenzalida H, Grilli A (1999) Isotopic composition and origin of precipitation in northern Chile. Appl Geochem 14:411-422

Bartlett MG, Chapman DS, Harris RN (2006) A decade of ground-air temperature tracking at Emigrant Pass Observatory, Utah. J Clim 19:3722-3731

Beard KV, Pruppacher HR (1971) A wind tunnel investigation of the rate of evaporation of small water drops falling at terminal velocity in air. J Atmos Sci 28:1455-1464

Berner RA, Kothavala Z (2001) Geocarb III: a revised model of atmospheric CO_2 over Phanerozoic time. Am J Sci 301:182-204

Bershaw J, Garzione CN, Higgins P, MacFadden BJ, Anaya F, Alveringa H (2006) The isotopic composition of mammal teeth across South America: A proxy for paleoclimate and paleoelevation of the Altiplano: EOS, Transactions, American Geophysical Union 87:Abstract #T33C-0519

Birkeland PW (1984) Soils and Geomorphology. Oxford University Press, New York

Blisniuk PM, Stern LA (2005) Stable isotope paleoaltimetry---a critical review. Am J Sci 305:1033-1074

Blisniuk PM, Stern LA, Chamberlain CP, Idleman B, Zeitler PK (2005) Climatic and ecologic changes during Miocene surface uplift in the southern Patagonian Andes. Earth Planet Sci Lett 230:125-142

Broccoli AJ, Manabe S (1992) The effects of orography on midlatitude Northern Hemisphere dry climates. J Climate 5:1181-1201

Came R, Veizer J, Eiler JM (in review) Surface temperatures of the Paleozoic ocean based on clumped isotope thermometry. Nature: in review **(UPDATE?)**

Cerling TE (1984) The stable isotopic composition of modern soil carbonate and its relation to climate. Earth Planet Sci Lett 71:229-240

Cerling TE, Quade J (1993) Stable carbon and oxygen isotopes in soil carbonates. *In:* Continental Indicators of Climate. Swart P, McKenzie JA, Lohman KC (eds) Proceedings of Chapman Conference, Jackson Hole, Wyoming, American Geophysical Union Monograph 78:217-231

Cerling TE, Harris JM, MacFadden BJ, Ehleringer JR, Leakey MG, Quade J, Eisenman V (1997) Global vegetation change through the Miocene/Pliocene boundary. Nature 389:153-157

Chadwick OA, Sowers JM, Amundson RA (1988) Influence of climate on the size and shape of pedogenic crystals. Soil Sci Soc Am J 53:211-219

Cross SL, Seltzer GO, Fritz SC, Dunbar RB (2001) Late Quaternary climate change and hydrology of tropical South America inferred from an isotopic and chemical model of Lake Titicaca, Bolivia and Peru. Quat Res 56:1-9

Currie BS, Rowley DB, Tabor NJ (2005) Middle Miocene paleoaltimetry of southern Tibet: implications for the role of mantle thickening and delamination in the Himalayan orogen. Geology 33(3):181-184

Cyr AJ, Currie BS, Rowley DB (2005) Geochemical evaluation of Fenghuoshan Group Lacustrine carbonates, north-central Tibet: implications for paleoaltimetry of the Eocene Tibetan Plateau. J Geol 113:517-533

Davidson GR (1995) The stable isotopic composition and measurement of carbon in soil CO_2. Geochim Cosmochim Acta 59(12):2485-2489

DeCelles PG, Horton BK (2003) Early to middle Tertiary foreland basin development and the history of Andean crustal shortening in Bolivia. Geol Soc Am Bull 115(1):58-77

DeCelles PG, Gehrels G, Quade J, Ojha TP (1998) Eocene-early Miocene foreland basin development and the history of Himalayan thrusting, western and central Nepal. Tectonics 17(5):741-765

DeCelles PG, Quade J, Kapp P, Fan M, Dettman DL, Ding L (2007a) High and dry in central Tibet during the late Oligocene. Ear Planet Sci Lett 253:389-401

DeCelles PG, Kapp P, Ding L, Gehrels GL (2007b) Late Cretaceous to middle Tertiary basin evolution in the central Tibetan Plateau: Changing environments in response to tectonic partitioning, aridification, and regional elevation gain. Geol Soc Am Bull 119(5-6):654-680

Dettman DL, Kohn MJ, Quade J, Ryerson FJ, Ojha TP, Hamidullah S (2001) Seasonal stable isotope evidence for a strong Asian monsoon throughout the past 10.7 Ma. Geology 29:31-34

Deutz P, Montanez IP, Moger HC (2002) Morphology and stable and radiogenic isotope composition of pedogenic carbonates in late Quaternary relict soils, New Mexico, USA: an integrated record of pedogenic overprinting. J Sediment Res 72:809-822

Dutton A, Wilkinson BH, Welker JM, Bowen G, Lohmann KC (2005) Spatial distribution and seasonal variation in $^{18}O/^{16}O$ of modern precipitation and river water across the coterminous USA. Hydrological Processes 19:4121-4146

Eiler JM, Schauble E (2004) $^{18}O^{13}C^{16}O$ in Earth's atmosphere. Geochim Cosmochim Acta 68:4767-4777

Eiler JM, Garzione C, Ghosh P (2006) Response to comment on "Rapid uplift of the altiplano revealed through ^{13}C-^{18}O bonds in paleosol carbonates. Science 314:5800

Ekart DD, Cerling TE, Montanez IP, Tabor NJ (1999) A 400 million year carbon isotope record of pedogenic carbonate: implications for paleoatmospheric carbon dioxide. Am J Sci 299: 805-827

Fox D, Koch PL (2004) Carbon and oxygen isotopic variability in Neogene paleosol carbonates: constraints on the evolution of C_4 grasslands. Palaeogr Palaeocl Palaeoecol 207:305-329

Friedman I, Smith GI, Gleason JD, Warden A, Harris JM (1992) Stable isotope composition of waters in southeastern California 1. modern precipitation. J Geophys Res 97(D5):5795-5812

Fritz P, Suzuki O, Silva C, Salati E (1981) Isotope hydrology of groundwater in the Pampa del Tamarugal, Chile. J Hydrol 53:161-184

Garzione CN, Quade J, DeCelles PG, English NB (2000a) Predicting paleoelevation of Tibet and the Himalaya from $\delta^{18}O$ versus altitude gradients in meteoric water across the Nepal Himalaya. Earth Planet Sci Lett 183:215-229

Garzione CN, Dettman DL, Quade J, DeCelles PG, Butler RF (2000b) High times on the Tibetan Plateau: paleoelevation of the Thakkola graben, Nepal. Geology 28:339-342

Garzione CN, Dettman DL, Horton BK (2004) Carbonate oxygen isotope paleoaltimetry: evaluating the effect of diagenesis on paleoelevation estimates for the Tibetan plateau. Palaeogeog Palaeoclim Palaeoec 212:119-140

Garzione CN, Molnar P, Libarkin JC, MacFadden BJ (2006) Rapid late Miocene rise of the Bolivian Altiplano: Evidence for removal of mantle lithosphere. Earth Planet Sci Lett 241:543-556

Ghosh P, Adkins J, Affek H, Balta B, Guo W, Schauble EA, Schrag D, Eiler JM (2006a) ^{13}C-^{18}O bonds in carbonate minerals: A new kind of paleothermometer. Geochim Cosmochim Acta 70:1439-1456

Ghosh P, Eiler JM, Garzione C (2006b) Rapid uplift of the Altiplano revealed in abundances of ^{13}C–^{18}O bonds in paleosol carbonate. Science 311:511-515

Gile LH, Peterson FF, Grossman RB (1966) Morphological and genetic sequences of carbonate accumulation in desert soils. Soil Sci 101:347-360

Gonfiantini R, Stichler W, Rozanski K (1995) (**ARTICLE TITLE?**) *In:* IAEA-TECDOC-825, Reference and intercomparison materials for stable isotopes of light elements. IAEA, Vienna. p. 13-30

Gonfiantini R, Roche M-A, Olivry J-C, Fontes J-C, Zupi GM (2001) The altitude effect on the isotopic composition of tropical rains. Chem Geol 181:147-167

Guo W, Eiler JM (2007) Evidence for methane generation during the aqueous alteration of CM chondrites. Meteoritics and Planetary Sciences in press **(UPDATE?)**

Hardy DR, Vuille M, Bradley RS (2003) Variability of snow accumulation and isotopic composition on Nevado Sajama, Bolivia. J Geophys Res 108 (D22):4693

Harris N (2006) The elevation history of the Tibetan Plateau and its implications for the Asian monsoon. Palaeogeogr Palaeoclim Palaeoecol 24:4-21

Hays PD, Grossman EL (1991) Oxygen isotopes in meteoric calcite cements as indicators of continental paleoclimate. Geology 19:441-444

Hernández R, Jordan T, Dalenz Farjat A, Echavarría L, Idleman B, Reynolds J (2005) Age, distribution, tectonics and eustatic controls of the Paranense and Caribbean marine transgressions in southern Bolivia and Argentina. J South Am Earth Sci 19:495-512

Hillel D (1982) Introduction to Soil Physics. Academic Press, New York

Hoorn C (2006) The birth of the mighty Amazon. Scientific American 294:52-59

Horton BK, Hampton BA, Lareau BN, Baldellon E (2002) Tertiary provenance history of the northern and central Altiplano (Central Andes, Bolivia); a detrital record of plateau-margin tectonics, J Sedimentary Res 72:711-726

Hsieh JCC, Chadwick O, Kelly E, Savin SM (1998) Oxyen isotopic composition of soil water: quantifying evaporation and transpiration. Geoderma 82:269-293

Hulka C (2005) Sedimentary and tectonic evolution of the Cenozoic Chaco foreland basin, southern Bolivia (Ph. D. dissertation), Freien Universität, Berlin

Jenny H, Leonard C (1934) Functional relationships between soil properties and rainfall. Soil Sci 38:363-381
Kay RF, MacFadden BJ, Madden RH, Sandeman H, Anaya F (1998) Revised age of the Salla beds, Bolivia, and its bearing on the age of the Deseadan South American Land Mammal "Age." J Vert Paleont 18:189-199
Kennan L, Lamb S, Rundle C (1995) K-Ar dates from the Altiplano and Cordillera Oriental of Bolivia - implications for Cenozoic stratigraphy and tectonics. J South Am Earth Sci 8:163-186
Kent-Corson ML, Sherman LS, Mulch A, Chamberlain CP (2007) Cenozoic Topographic and climatic response to changing tectonic boundary conditions in western North America. Earth Planet Sci Lett: in press **(UPDATE?)**
Kim S-T, O'Neil JR (1997) Equilibrium and non-equilibrium oxygen isotope effects in synthetic carbonates. Geochim Cosmochim Acta 61:3461-3475
Koch PL, Zachos JC, Dettman DL (1995) Stable-isotope stratigraphy and paleoclimatology of the paleogene bighorn basin (Wyoming, USA). Palaeogeogr Palaeoclim Palaeoecol 115:61-89
Kroon D, Steens T, Troelstra SR (1991) Onset of monsoonal related upwelling in the western Arabian Sea as revealed by planktonic foraminifers. *In:* Proceedings of the Ocean Drilling Project, Scientific Results. Prell WL, Niitsuma N (eds) 117:257-263
Lakhanpal RN (1970) Tertiary floras of India and their bearing on historical geology of the region. Taxon 19(5):675-694
Larrain H, Velazquez F, Cereceda P, Espejo R, Pinot R, Osses P, Schemenauer RS (2002) Fog measurements at the site "Falde Verde" north of Chanaral compared with other fog stations of Chile. Atmos Res 64:273-284
Latorre C, Quade J, McIntosh WC (1997) The expansion of C_4 grasses and global change in the late Miocene: stable isotope evidence from the Americas. Earth Plan Sci Lett 146:83-96
Leier AL (2005) The Cretaceous evolution of the Lhasa terrane, southern Tibet, Ph.D. Dissertation, Univ. of Arizona
Liu B, Phillips FM, Campbell AR (1996) Stable carbon and oxygen isotopes of pedogenic carbonates, Ajo Mountains, southern Arizona: implications for paleoenvironmental change. Palaeogr Palaeocl Palaeoecol 124:233-246
Machette MA (1985) Calcic soils of the southwestern United States. *In:* Soils and Quaternary Geology of the Southwestern United States. Weide DL, Faber ML (eds) Geol Soc Am Spec Pap 203:1-21
MacFadden BJ, Campbell KE Jr, Cifelli RL, Siles O, Johnson NM, Naeser CW, Zeitler PK (1985) Magnetic polarity stratigraphy and mammalian fauna of the Deseadan (late Oligocene early Miocene) Salla beds of northern Bolivia. J Geol 93:223-250
Marshall LG, Swisher CC III, Lavenu A, Hoffstetter R, Curtis GH (1992) Geochronology of the mammal-bearing late Cenozoic on the northern Altiplano, Bolivia. J South Am Earth Sci 5(1):1-19
Mulch A, Teyssier C, Cosca MA, Vanderhaeghe O, Vennemann V (2004) Reconstructing paleoelevation in eroded orogens. Geology 32:525-528
Pagani M, Freeman KH, Arthur MA (1999) Late Miocene atmospheric CO_2 concentrations and expansion of C_4 grasses. Science 285:876-879
Pagani M, Zachos J, Freeman KH, Bohaty S, Tipple B (2005) Marked change in atmospheric carbon dioxide concentrations during the Oligocene. Science 309:600-603
Pearson PN, Palmer MR (2000) Atmospheric carbon dioxide concentrations over the past 60 million years. Nature 406:695-699
Poage MA, Chamberlain CP (2001) Empirical relationships between elevation and the stable isotope composition of precipitation and surface waters: consideration for studies of paleoelevation change. Am J Sci 301:1-15
Quade J, Cerling TE (1995) Expansion of C_4 grasses in the late Miocene of northern Pakistan: evidence from stable isotopes in paleosols. Palaeogr Palaeocl Palaeoecol 115:91-116
Quade J, Cerling TE, Bowman JR (1989a) Systematic variation in the carbon and oxygen isotopic composition of Holocene soil carbonate along elevation transects in the southern Great Basin, USA. Geol Soc Am Bull 101:464-475
Quade J, Cerling TE, Bowman JR (1989b) Development of the Asian Monsoon revealed by marked ecological shift in the latest Miocene in northern Pakistan. Nature 342:163-166
Quade J, Cater JML, Ojha TP, Adam J, Harrison TM (1995) Dramatic carbon and oxygen isotopic shift in paleosols from Nepal and late Miocene environmental change across the northern Indian sub-continent. Geol Soc Am Bull 107:1381-1397
Quade J, Rech J, Latorre C, Betancourt J, Gleason E, Kalin-Arroyo M (2007) Soils at the hyperarid margin: the isotopic composition of soil carbonate from the Atacama Desert. Geochim Cosmochim Acta, in press **(UPDATE?)**
Ramesh R, Sarin MM (1995) Stable isotope study of the Ganga (Ganges) river system. J Hydrol 139:49-62
Rech JA, Currie BS, Michalski G, Cowan AM (2006) Neogene climate change and uplift in the Atacama Desert, Chile. Geology 34(9):761-764

Roe GH (2005) Orographic precipitation. Ann Rev Earth Planet Sci 33:645-671
Roperch P, Herail G, Fornari M (1999) Magnetostratigraphy of the Miocene Corque Basin, Bolivia; implications for the geodynamic evolution of the Altiplano during the late Tertiary. J Geophys Res 104(9):20415-20429
Rowley DB, Pierrehumbert RT, Currie BS (2001) A new approach to stable isotope-based paleoaltimetry: implications for paleoaltimetry and paleohypsometry of the High Himalaya since the Late Miocene. Earth Planet Sci Lett 188:253-268
Rowley DB, Currie BS (2006) Palaeo-altimetry of the late Eocene to Miocene Lunpola basin, central Tibet. Nature 439:677-681
Rowley DB, Garzione CN (2007) Stable isotope-based Paleoaltimetry. Annu Rev Earth Planet Sci (in press) **(UPDATE?)**
Royer D (1999) Depth to pedogenic carbonate horizon as a paleoprecipitation indicator? Geology 27:1123-1126
Rozanski K, Sonntag C (1982) Vertical distribution of deuterium in atmospheric water vapour. Tellus 34:135-141
Ruddiman WF, Raymo ME, Prell WL, Kutzbach JE (1997) The climate uplift-connection. *In:* Tectonic Uplift and Climate Change. Ruddman WL (ed) Plenum Press. p 3-15
Salomans W, Goudie A, Mook WG (1978) Isotopic composition of calcrete deposits from Europe, Africa and India. Earth Surf Processes 3:43-57
Santrock J, Studley SA, Hayes JM (1985) Isotopic analysis based on the mass-spectrum of carbon-dioxide. Anal Chem 57:1444-1448
Savin SM, Douglas RG, Stehli FG (1975) Tertiary marine paleotemperatures. Geol Soc Am Bull 86:1499-1510
Schauble EA, Ghosh P, Eiler JM (2006) Preferential formation of ^{13}C-^{18}O bonds in carbonate minerals, estimated using first-principles lattice dynamics. Geochim Cosmochim Acta 70:2510-2529
Siegenthaler U, Oeschger, H (1980) Correlation of ^{18}O in precipitation with temperature and altitude. Nature 285:314-17
Smith AG, Hurley AM, Briden JC (1981) Phanerozoic paleocontinental world maps, Cambridge, UK, Cambridge University Press, 102 p
Stern, LA, Chamberlain, CP, Reynolds, RC, Johnson GD (1997) Oxygen isotope evidence of climate changes from pedogenic clay minerals in the Himalayan molasses. Geochim Cosmochim Acta 61:731-744
Stern LA, Blisniuk PM (2002) Stable isotope composition of precipitation across the southern Patagonian Andes. J Geophys Res 107(D23): doi:10.1029/ 2002JD002509
Stewart MK (1975) Stable isotope fractionation due to evaporation and isotopic exchange of falling waterdrops—applications to atmospheric processes and evaporation of lakes. J Geophys Res 80:1133-1146
Talbot MR (1990) A review of the paleohydrological interpretation of carbon and oxygen isotopic ratios in primary lacustrine carbonates. Chem Geol 80:261-279
Talma AS, Netterberg F (1983) Stable isotope abundances in calcretes. *In:* Residual Deposits: Surface Related Weathering Processes and Materials. Wilson, RCL (ed) Oxford: Blackwell Scientific Publ., p 221-233
Tian L, Masson-Delmotte V, Stievenard M, Tao T, Jouzel J (2001) Tibetan Plateau summer monsoon northward extent revealed by measurements of water stable isotopes. J Geophys Res 106:28,081-28,088
Tian L, Yao T, White JWC, Yu W, Wang N (2005) Westerly moisture transport to the middle of Himalayas revealed from the high deuterium excess. Chinese Sci Bull 50:1026-130
Uba CE, Heubeck C, Hulka C (2006) Evolution of the late Cenozoic Chaco foreland basin, southern Bolivia. Basin Res 18:145-170
Veizer J, Ala D, Azmy K, Bruckschen P, Buhla D, Bruhn F, Carden GAF, Diener A, Ebneth S, Godderis Y, Jasper T, Korte C, Pawellek F, Podlaha OG, Strauss H (1999) $^{87}Sr/^{86}Sr$, $\delta^{13}C$ and $\delta^{18}O$ evolution of Phanerozoic seawater. Chem Geol 161:59-88
Vuille M, Bradley RS, Werner M, Healy R, Keimig F (2003) Modeling $\delta^{18}O$ in precipitation over the tropical Americas: 1. Interannual variability and climatic controls. J Geophys Res 108: doi:10.1029/ 2001JD002038
Wang ZG, Schauble EA, Eiler JM (2004) Equilibrium thermodynamics of multiply substituted isotopologues of molecular gases. Geochim Cosmochim Acta 68:4779-4797
Wolfe BB, Aravena R, Abbott MB, Seltzer GO, Gibson JJ (2001) Reconstruction of paleohydrology and paleohumidity from oxygen isotope records in the Bolivian Andes. Palaeogeogr Palaeoclimatol Palaeoecol 176(1-4):177-192
Wynn JG (2004) Influence of Plio-Pleistocene aridification on human evolution: evidence from paleosols of the Turkana Basin. Am J Phys Anthro 123:106-118
Zachos J, Pagani M, Sloan L, Thomas E, Billups K (2001) Trends, rhythms, and aberrations in global climate 65 Ma to present. Science 292:686-693
Zhang X, Nakawo M, Yao T, Han J, Xie Z (2002) Variations of stable isotopic compositions in precipitation on the Tibetan Plateau and its adjacent regions. Science in China (Series D) 25(6):481-493